COTS GNSS Receiver

Testing of an on-board receiver for the Indian Space Research Organisation satellite INS-1C

Sander Vancraen 4057856

THESIS
Master Spacefligth

TU Delft Delft University of Technology

Aerospace Engineering

March 1, 2021

Acknowledgments

Space exploration has been a passion for me since I was a young child. The magazines EOS and Quest were my favorite reading material and made me interested to go study at the TU-Delft. My years at the TU-Delft were fascinating. Especially the group projects were highly motivating, interesting and fun for me.

Making a thesis was the ultimate challenge for me as a seriously dyslexic and dis-orthographic student. It really was the toughest period of my life as I ran into some major disappointments during the execution. It proved to be impossible, for reasons explained in the thesis, to get hold of a space-ready dual frequency COTS receiver to make the tests much more relevant. Also, we expected data from the INS-1B satellite as a basis for reference and validation from a real mission. Unfortunately, contact to this satellite was lost before any relevant data could be transmitted during the first months of my work. However, I hope I can contribute with the tests executed in this thesis to the preparatory works for future space missions with GNSS receivers at the Indian Space Research Organization.

This work would never have come to good ending without the great support from my thesis advisor Dr. Ir. Wouter Van der Wal of the space exploration department of the TU-Delft. His guidance in the selection of the topic and in the daily elaboration of the work program have been essential. As this project was in collaboration with the Indian Space Research Organization (ISRO), the assistance of Phd. student Sujay Narayana was important to enable interfacing with ISRO. He also assisted to solve multiple technical problems along the way. Ir. Wim Simons has helped me a lot to get access to and understanding of GIPSY, an essential research tool in this work. Dr. Ir. Hans van der Marel was so kind to provide all the test equipment I needed.

I also would like to thank my fellow students Michael Van Den Broeck, René Hoogendoorn, Randy van Dooren and the many other students that shared the flex-rooms and that provided me with support, companionship and a nice working environment.

Last but not least, I want to thank my family that supported me through my entire school career and especially the years at TU-Delft. Due to my dyslexia their incessant support was indispensable and what kept me going till the finish!

Contents

List of Figures

List of Tables

List of Symbols

G_r	Atenna gain receiver.
G_s	Atenna gain satellite.
L	Signal loss.
L_p	Antenna back-to-front ratio.
M_{db}/Hz	Link margin.
NF	Noise figure.
P_s	Atenna power satellite.
R	Distance.
RC	Radius of Curvature.
R_{bf}	Antenna back-to-front ratio.
T_0	Reference temperature.
T_a	Antenna noise temperature.
T_{sky}	Clear sky temperature.
T_s	Receive system noise temperature.
Γ_r	Antenna reflection coefficient receiver.
Γ_s	Antenna reflection coefficient satellite.
α	Atmospheric loss.
$\frac{C}{N_0}$	The Signal to (reference) noise ratio.
λ	Carrier wavelength.
a	Semi major axis.
c	Speed of light.
e	Eccentricity.
f_c	Carrier frequency.
h	Height.
k	Boltzmann constant.
lat	latitude.
lon	longitude.
p	Polarization match.

List Of Abbreviations

BINEX	BINary EXchange.
C/A	Coarse/Acquisition.
CANX	Canadian Advanced Nanospace eXperiment.
CAS	Chinese Academy of Science.
CNR	Carrier-to-noise ratio.
COCOM	Coordinating Committee for Multilateral Export Controls.
CODE	Center for Orbit Determination Europe.
COTS	Commercial Off The Shelf.
DOP	Dilution of Precision.
DSE	Design Synthesis Exercise.
ECMWF	European Centre for Medium-Range Weather Forecasts.
EMI	Electro Magnetic Interference.
ESA	European Space Agency.
GEO	geosynchronous satellite.
GIM	Global Ionospheric Map.
GLONASS	GLObal NAvigation Satellite System.
GNSS	Global Navigation Satellite System.
GPS	Global Positioning System.
GRAS	GNSS Receiver for Atmospheric Sounding.
IACC	Iononspheric Analyses Centers.
IGS	International GNSS Service working group.
INS	Indian Nano Satellite.
IRNSS	Indian Regional Navigation Satellite System.
ISRO	Indian Space Research Organisation.
JPL	Jet Propulsion Laboratory.
LEO	Low Earth Orbit.
LNA	Low-Noise Amplifier.
NASA	National Aeronautics and Space Administration.
NRCan	Natural Resource Canada.
PDOP	Positional Dilution of Precision.
POD	Precise Orbit Determination.
PPP	Precise Point Positioning.
PSLV	Polar Satellite Launch Vehicle.
QZSS	Quasi-Zenith Satellite System.
RINEX	Receiver Independent Exchange Format.
rms	root mean square.
SBAS	Satellite-Based Augmentation Systems.
SNR	Signal-to-noise ratio.

STK	Systems Tool Kit.
TEC	Total Electron Content.
TID	Total Ionizing Dose.
TLE	Two-Line Element set.
TTFF	Time To the First position Fix.
UPC	Polytechnic University of Catalonia.
WGS84	World Geodetic System 1984.
WHU	Wuhan University.

Abstract

The Indian Space Research Organisation(ISRO) plans to equip future satellites of its Indian Nano Satellite (INS) with COTS dual frequency receivers in order to let them contribute to various scientific research opportunities. This thesis develops a test framework for Commercial Off The Shelf (COTS) Global Navigation Satellite System (GNSS)receivers on Nano satellites of the Indian Space Research Organisation(ISRO) to be used for scientific applications. This thesis aims to provided answer to the suitability of this data for scientific application.

We have analyzed that the current generation Skytraq single frequency receiver, mounted in previous INS-1A to INS-1C missions, has with an accuracy in the meters range insufficient position accuracy to be used for scientific applications. Nevertheless, based on historical mission experiences and design constraints, a receiver-antenna system selection has been executed. Using this system as an example configuration, a test framework has been setup to analyze influential design and system configuration parameters influence on the GNSSreceivers for future missions. The test setup consist of a series of static tests that enable to research the hardware configuration, such as the influence of a ground plane, and the data processing options, such as filters for the data and the choice of atmospheric models. It is complemented with a dynamic analysis of the receiver simulated performance in orbit using a GNSS simulator.

Multiple data series were obtained for each individual test of the framework. These data series were analyzed with a developed data handling protocol in which multiple data processing software packages were used. In order to obtain comparable results in all test series, average deviations of the position fixes in the test periods were calculated and analyzed. This leads to a number of conclusions: The current antenna mounting on INS-1C is less than optimal and a ground plane would enhance the antenna performance with 20%. The raw data are essential for scientific experiments. However, they can most likely be limited to those obtained from GPS satellites excluding GLONASS and other GNSS constellations. It does pay off to include low viewing angle measurements for optimal results. The ionospheric models are indispensable to achieve sub meter accuracy with single frequency receivers.

Given the sub meter accuracy level that can already be obtained with a Skytraq single frequency receiver it is likely that a future dual frequency version will allow centimeter accuracy level of the position data which would allow for a range of scientific applications. It will be possible to use the test framework to assess our principal question whether COTS receiver could contribute to scientific research.

1 Introduction

In this chapter we will give an overview of the scientific background and the context in which this master thesis work has been executed. Accurate space born GNSS receivers contribute to multiple fields of research. An increase of the GNSS receiver capabilities with a sufficient accuracy for research purposes at low costs with COTS GNSS receivers has potential to progress this research faster. We will investigate conditions and configurations to enable the use of COTS GNSS receivers for nano satellites in LEO orbits in this work. We will give a brief overview of past missions that are relevant to the research topic. This work relates to future missions of the Indian Space Research Organisation (ISRO) of which the nano satellite program will be described. As accuracy of position measurements is crucial for those research topics, we will provide an extensive overview of all error sources and their potential mitigation methods that can be applied. We will end with the problem description and the research questions that are being addressed in this work.

1.1 Research with Dual-Frequency GNSS receivers

This study is doing groundwork to investigate what benefits could be expected if dual frequency COTS GNSS receivers could be used in the INS program of ISRO. We want to give an idea of the research possibilities that could arise from its use. The main addressable research fields are the Thermosphere, Ionosphere and Gravitation.

1.1.1 Thermosphere and Ionosphere Research

The thermosphere is a region of the Earth's atmosphere above the mesosphere and below the exosphere, roughly situated between 85 km and 600 km above the Earth[1]. It is the region in which most of the Low-Earth orbit satellites are situated, including the satellites relevant for this study. The thermosphere is an extremely hot and changing area of our atmosphere, hence the name. It contains highly diluted gas that can reach temperatures exceeding 2500 ° C[1].

The Ionosphere overlaps with the thermosphere, it extends vertically from the mesosphere ($\sim$ 50 km) to the upper exosphere at approximately 1000 km. It contains highly ionized gas that originates from photoionozation of molecules caused by ultra violet radiation from the sun [1]. This has an important practical consequence: it influences radio propagation when signals travel through, along different paths, to places on the Earth.

The ionosphere, because of its electromagnetic properties, causes deformation of radio-waves and hence the GNSS signals. Thanks to the signal deformations, we can reverse engineer from these deformations some properties of the composition of the ionosphere through which the signals passed. GNSS receivers can help to determine the electron density of the ionosphere. This only can be done with a dual frequency receiver. Different radiofrequencies are affected differently by the ionosphere. By tracking the two different GPS frequencies L1 and L2 one can determine the Total Electron Content (TEC). Since both signals travel along exactly the same path their phase and frequency shifts can be calculated[2].

The ionosphere is a continuously changing environment, real time information of the ionosphere is an area of interest for multiple applications. For instance, it can be used for the correction of GNSS signals itself but also other applications that use radio communication, for example in civil aviation. For this

purpose multiple agencies such as European Space Agency (ESA) and National Aeronautics and Space Administration (NASA) publish daily forecasts of the ionospheric weather conditions[3].

While the satellite travels through the thermosphere, it experiences the density variations in the thermosphere. These density variations will cause a difference in drag on the satellite resulting in a variation in its travel speed. With the help of precise positioning measurements these speed variations can be observed and used to model the density variations. These density variations are also useful for the space weather forecasts.

Another orbit disturbance that can be monitored through the velocity changes is the power of the solar radiation. Depending on the orientation towards the Sun solar radiation has varying strength, which causes different accelerations or decelerations of the satellite. In other words, precise position determination of the satellite can tell us something about solar radiation pressure experienced by the satellite. The estimation of this solar pressure can be used to calculate the effect on other satellites in its vicinity.

As these velocity effects are intertwined, it will always be necessary to model or measure with alternative methods several of the effects in order to deduce the effect of interest.
The benefit of using space born dual frequency COTS receivers, compared to purpose build GNSS receivers and other instruments, is that they provide additional measurements in a cost effective way. These can be used for ionospheric and thermosphere weather observation and prediction. Given the cheap nature of these receivers and their increasing miniaturization, they can be a limited extra payload for many missions, making those more useful.

1.1.2 Gravitation Research

This section will provide some insights in the domain of gravitation research and what COTS GNSS receivers could potentially contribute to this research field.

The Earth‘s gravitational field is not uniform due to all kinds of topographic irregularities as well as internal density differences. The gravitation is not only varying over the surface of the earth, it is also dynamically changing over time [4] [5] [6]. The non-uniform nature of the gravitation field, is the subject of many scientific studies such as [4] [5] [6]. It can tell us much about the Earth, ranging from internal mechanisms such a mantle flow to variations in ice thickness due to climate change[6].

Changes in the gravitation field are happening in different time frames. There are very short term effects of repetitive or non-repetitive nature. The effect of tides in the oceans is repetitive. Weather phenomena such as thunderstorms can have a completely irregular effect in the order of magnitude of hours. Although these effects are influencing the measurements made by satellites based on the GNSS receivers, there are much better methods to observe them. So it will rather be that these alternative methods are used to correct the GNSS data. These corrected GNSS data can then be used for other purposes such as those described in the previous paragraph.

Some changes in the gravitation field are happening over a very long period of time, for instance the tectonic plate movements. Those are also not relevant for satellite based GNSS receiver based observation, given the very limited changes, too small to measure, during the lifetime of the satellites.

Phenomena impacting the Earth gravity field with significant variation over several months to years are most suited for observations with GNSS based satellite receivers. Examples of these phenomena are the seasonal changes of large river basins such as the Congo river and Amazon river. Effects with a longer time span are for instance the changes in the ice thickness on the Antarctic continent due to climate change.

The methods used for this kind of observations are based on velocity and/or position changes of the satellite compared to a theoretical orbit that does not contain any gravitational irregularities. In order

to obtain a deviation that is only influenced by gravitation, all other effects have to be filtered out. This requires the filtering of the influence by solar radiation pressure and mainly aerodynamic drag. From the velocity changes, after filtering out the effects caused by the thermosphere described above, the gravity variations are derived. These gravity variations in themselves should be filtered, for instance to remove tidal effects. The more accurate the velocity changes can be measured with a dual frequency GNSS receiver, the more phenomena can be analysed.

The benefit of using satellite GNSS receiver based measurements is that they allow in a cost effective way to measure phenomena over very large areas, compared to terrestrial measurements that can only cover limited area's. They allow for measuring phenomena that are hard to spot on the surface, such as the distribution of water underground. The disadvantage of using GNNS measurements in gravitational research is that it is only suitable to investigate long-wavelength part of the gravity field. Short-wavelength observations require additional instrumentation. This is why missions like GRACE opted to also include, for instance, inter-satellite ranging between GRACE A and B [7]. Including Short-wavelength gravitational measurements allows the visualization of more temporal phenomena, such as weather changes.

1.2 GNSS Measurement errors

The measurements of GNSS signals are influenced by several types of (random) errors. These errors can be divided into three categories based on the location where they occur: receiver based errors, satellite based errors and propagation medium errors [8] [9] [2]. An overview of the various error types and corresponding magnitudes is provided in table 1.1.

1.2.1 Receiver based errors

GNSS receivers mainly use two methods for their position calculations. One is based on the decoding of the coded message sent by the GNSS satellite, which is then used for the position calculation. The other method is based on the measurement of the deformation of the carrier phase of the signal sent by the GNSS satellites. Depending on the method used, the influence of different error sources may vary significantly. Errors induced in the GNSS receiver are: receiver measurement noise, receiver clock error, multipath error and receiver instrumental bias [2].

Receiver measurement noise consists of the following sources : Thermal noise induced by amplifiers, antenna-cables and the receiver hardware all contribute to the random thermal noise[2]. Thermal noise is the electronic noise generated by the thermal agitation of the charge carriers, the electrons inside an electrical conductor at equilibrium. This agitation happens regardless of any applied voltage. Interference from other signals similar to Global Positioning System (GPS) and quantization noise, originating from rounding and truncating errors in the receivers digital signal processing, correspondingly add to the receiver measurement noise. Code measurements tend to be more affected then phase measurements.

The **receiver clock error** is an additional parameter in the user position estimation algorithm. Four satellites are required to determine the GNSS receiver position in three dimensions as well as the receiver clock error, even then there always remains a residual error.

Multipath error is caused by reflections from objects in the vicinity of the receiving antenna(s) causing the signal to arrive at the receiver via multiple paths. This can happen in applications on Earth due to the presence of buildings or other obstructions. In space applications, it are mostly the structures of the satellite itself that can be at the origin of this type of errors. The phase and amplitude are distorted as the reflected signals are superimposed on the desired direct-path signal. The multipath error affects code based measurements much more significantly with 2 orders of magnitude compared to carrier phase measurements, see table 1.1.

Analog hardware within the receiver causes an **instrumental bias error** due to the frequency dependent transmission delays. The differential instrumental bias is existent in dual frequency receivers and affects ionospheric delay measurements.

1.2.2 Satellite based errors

Errors that originate at the satellite consist of: instrumental bias errors, relativistic effects due to the dissimilar gravitational potential experienced by satellites, satellite clock errors and ephemeris errors.

The different frequency signals propagate through different analog circuitry before digitization implying that these signals undergo different propagation delays within the satellite causing **instrumental bias**. Each of the different GPS frequencies has an instrumental bias, the difference between these instrumental biases is known as differential instrumental bias. This is the same phenomenon as previously discussed for the receiver. The satellite's differential instrumental biases corrupt the ionospheric delay measurements obtained from a dual frequency receiver. Instrumental biases must be estimated and mitigated to obtain accurate estimates of the ionospheric delay.

The special and general theory of relativity predicts that the clocks used in the GNSS transmitter and receiver are affected by **relativistic effects**. The GNSS satellite clock runs at a different pace than the receiver clock due to difference in experienced gravitational potential. To compensate for the prescribed relativistic effects, the satellite clock frequency is adjusted to 10.22999999543 MHz before launch[2]. The user receiver is also required to make a correction for the periodic effect that arises due to the assumption of a circular orbit and its height. In reality, the elliptical orbit of GNSS satellites causes a time invariant gravitational potential and velocity.

GNSS satellites incorporate highly stable clocks that do not de-correlate spatially, but can de-correlate temporally. An error of about 8.64 to 17.29 ns per day is caused by the drift of the **satellites clock**. Each GNSS satellite clock is individual analyzed by a master control station to determine the clock error. The station transmits the value of the clock error to each individual GNSS satellite for rebroadcast in the navigation mission. The error for the Coarse/Acquisition (C/A) code pseudo-range observations is modelled as a 2nd degree polynomial[2].

Ephemeric errors are the errors that originate in inaccurate position knowledge of the GNSS satellites that are being tracked by the receiver. The inaccurate position knowledge is caused by un-modeled disturbances in the orbit of the GNSS satellite. New parameters to model the precise position are uploaded every few hours to GNSS satellites. Nevertheless, in between the updates there are new effects that can cause deviations. The order of magnitude of the remaining Ephemeric errors is small. This error is also going to be further reduced in the near future, at least for GPS. A planned update of the GPS groundstations will allow for continuous updating of the parameters required for the exact position calculation.

1.2.3 Errors due to propagation medium

The errors induced by delay of the GPS signal as it propagates through the layers of the atmosphere include the ionosphere and tropospheric delay. The tropospheric delay is non-existent for receivers placed in Low Earth Orbit (LEO). As indicated before, the ionosphere is a region in the atmosphere that consists of ionized gases free of electrons and ions extending from 50 to approximately 1000 km.[1], exactly where a LEO satellite is orbiting. The presence of free electrons in the ionosphere changes the velocity and direction of propagation of the GNSS signals. This effect delays the code phase measurements but advances the carrier phase measurements, the magnitudes are expressed in table 1.1.

The error caused by the tropospheric delay is one of the biggest error sources for measurements made on the Earth's surface[2]. The magnitude of this error is dependent on the weather conditions in the troposphere. Dry weather conditions are indicative of smaller tropospheric errors. Like for ionospheric

errors, the magnitude of the error varies with the distance the signal has to travel through the troposphere. In general the error in the signal for a satellite near zenith will be in the order of magnitude of 2 to 3 meter[2]. But signals that are low on the horizon can have a delay that increases up to 20 meter[2].

Table 1.1: Overview of various errors and corresponding magnitudes that would be found on a receiver a board a space craft [9][10][2]

	Single-frequency	Dual-frequency
Receiver clock error (m)	1.5	1.5
Multipath error (m)		
code based measurements	1-5	1-5
carrier-phase measurements	0.01 - 0.05	0.01 - 0.05
Receiver instrumental bias (m)	-	5.0
Receiver measurement noise (m)		
code based measurements	0.5	0.5
carrier-phase measurements	0.001 - 0.002	0.001 - 0.002
Ephemeris error (m)	1.5	1.5
Satellite clock error(m)	2.59 - 5.18	2.59 - 5.18
Satellite instrument bias (m)	0.55	1.5
Ionospheric delay (m)	1 - 15 (depending on elevation)	-
tropospheric delay	1-20 (depending on elevation)	1-20 (depending on elevation)

1.2.4 Dilution of precision

Apart from the measurement errors, the Dilution of Precision (DOP) is the introduction of an additional uncertainty in the position determination based on GNSS signals caused by the unequal distribution of tracked satellites across the field of view.
This unequal distribution can result in multiple satellites that are detected closely to one line of view from the detection point. In such situations the error margins of the different satellite signals overlap and the position uncertainty increases. This is illustrated in figure 1.1.

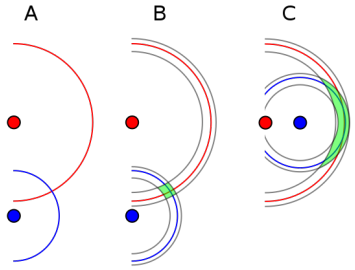

Figure 1.1: Example of Geometric Dilution Of Precision (GDOP) for simple Triangulation. Three different situations are shown: A) Triangulation. B) Triangulation with error. C) Triangulation with error and poor GDOP.[11]

1.3 Error Mitigation

Error Mitigation is important as the addition of all the different errors that influence the position determination on the basis of GNSS satellite signals would lead to deviations in the order of magnitude of many meters. This section describes a number of methods that can be used to reduce the error to centimetre level, which is required for most scientific applications.

1.3.1 Mitigation of Receiver-based Errors

Receiver-based errors happen in both single and dual frequency based systems. This category of errors is not mitigated by using a dual frequency system. The thermal noise, from the different components of the receiver system, induces a random error that is very hard to model and that cannot be corrected for. This is the most difficult category of errors to mitigate. The only way to limit this error is to reduce it to an insignificant level by selecting high quality components. For instance, the antenna cable needs to be selected as high quality as possible and it needs to be kept as short as possible. In the antenna selection the Low Noise Amplifier thermal noise figure is retained as an important trade-off criterion in the antenna selection section further in this work.

The interference from other signals sources can be prevented by taking care of proper Electro Magnetic Interference (EMI) shielding. Most COTS receivers come with housings that ensure already EMI-Shielding that is sufficient for cubesat applications. The receiver that will be selected in this mission has a sufficient EMI-Shielding provided by the manufacturer. Additionally, when a satellite designer is aware of potential sources of GNSS-like signals special precautions can be taken to shield those.

Quantization and truncation errors cannot be totally avoided, but they can be minimalized by using quantization algorithms for the GNSS signal that are as accurate as possible. This is limited by the capabilities of the receiver hardware. From the user perspective there is nothing that can be done about these errors. This choices are made by the manufacturer. It can be observed from table 1.1 that the receiver noise errors have the smallest contribution to all error sources and that quantization and truncation errors are the smallest component of this error. Therefore, this error can be neglected.

The receiver clock error consists of 2 components, a random error and a bias. The manufacturer can compensate for this bias. The random error can be partly corrected with software compensations implemented by the manufacturer, which are not made public. The clock error that is given in the datasheets is the one after the manufacturer‘s compensations. What remains of this error can no further be mitigated by the user, but since high accuracy of the receiver clock is not a requirement, this error has very limited consequences. The receiver that will be selected for this research has a clock error in the order of 10 nanoseconds as in indicated in appendix B. A mitigation method could be ussed to bring down the effect of the clock error is to use double differencing.

The techniques used to mitigate the multipath error can be classified in three categories: pre-receiver design measures, receiver signal processing and post-receiver signal processing. In general, several hardware precautions can be taken to prevent multipath from occurring in the first place. During the design process of the satellite, care should be taken that no objects are in the field of view of the antenna since these can cause signal reflections. Reflected signals coming from outside the field of view can be prevented by using a choke-ring design of the antenna. However, in a Cubesat space comes at a cost and in general the choke-ring design is too voluminous. In the specific case of the ISRO satellite, this is certainly the case. In this particular situation even a proper ground-plane is not available. This will be impacting the antenna gain and radiation pattern. It also increases the likelihood of multipath errors.

Modifying the tracking loop discriminator is a receiver signal processing technique to resist multipath signals. Post processing software, such as GIPSY can filter out multipath signals by analyzing unexpected time delays in GNSS satellites that are tracked over longer periods of time. This is a feature of GIPSY that is used in all future tests.

Frequency dependent delays caused by the analog hardware in dual frequency receivers can be estimated by techniques based on Kalman filtering and least squares adjustment methods. Manufacturers can do laboratory testing to quantify the difference in delays of different frequencies. This is an expensive process and it is generally not done for COTS receivers due to the very small nature of this error. This error is normally in the range of a few centimeters. However, this error affects the accuracy of the ability of dual frequency receivers to correct for the ionospheric error. This will be further explained in the context of Ionospheric errors below. An important sidenote related to this error is that it causes a structural weakness in the GLONASS system approach. GLONASS uses 14 different frequencies to broadcast its signals. This introduces 14 different analog frequency errors, making the entire modelling of the frequency dependent delays more complex. Corrections for the instrumental bias are normally taken into account in the software of the receivers.

1.3.2 Satellite based error mitigation

Each of the different frequency signals emitted by the satellite experiences a different instrumental bias inside the satellite. The difference in delay caused by these instrumental biases is known thanks to pre-launch measurements. This known difference can be used to correct for the instrumental biases for the different signals. This variation is the most important component of this error because it causes problems for the determination of the ionospheric error when using a dual frequency approach as will be explained later. The absolute instrumentation bias is harder to accurately estimate, a similar method as the one which enabled to determine the receiver instrument error can be used. Similar to receiver instrumental errors, these satellite instrumental bias errors are compensated for in the software of the receivers.

The error caused by the relativistic effect on the clock of the GNSS satellite is already compensated for by a satellite clock frequency adjustment to 10.22999999543 MHz before launch[2]. The user receiver makes a correction for the periodic effect that arises due to the assumption of a circular orbit that is not correct.

The base for ephemeris errors can be eliminated in post-processing calculations because at the time of the post processing, accurate positions of the GNSS satellites are known to these programs. This is possible thanks to work of institutions such as International GNSS Service working group (IGS) as will be explained in the next section. Their data are then used in post processing programs which will be discussed in the next chapter.

Given that the exact positions of GNSS satellites are extremely important for all kinds of calculations, their positions are tracked by at least 3 ground stations around the globe. They monitor disturbances of the GNSS satellites orbit.

1.3.3 Mitigation of errors due to the propagation medium

The Ionospheric error is the biggest error source. It can be mitigated using 2 approaches or a combination of both. The first mitigation approach is to use ionospheric models, which we will use extensively in this work; the second is by applying multiple frequency receivers.

Different ionospheric models are made by various research groups. The biggest of those is the IGS. This group contains seven associated Iononspheric Analyses Centers (IACC) : The Center for Orbit Determination Europe (CODE), The European Space Agency (ESA), Jet Propulsion Laboratory (JPL) associated with NASA, Polytechnic University of Catalonia (UPC), Natural Resource Canada (NRCan), the Chinese Academy of Science (CAS) and Wuhan University (WHU). Together they compose the Global Ionospheric Map (GIM), which is updated every 2 hours. This is a weighted map of the various IACCs maps. The GIM map provides a spatial resolution of 2.5 by 5 degrees and a temporal resolution of 2 hours. This resolution is expected to improve over time.

The GIM model is based on continuous observations of more than 400 GNSS research stations. It has been made every day since 1998. There are three versions of this model available :

- One version with a latency of less than 24 hours
- One final version available after approximately 11 days
- One forecast version which is provided 2 days in advance of a certain date.

It is important when processing data to be aware of the fact that the final version is offering more accurate calculations than the earlier version. Nevertheless the accuracy of the model remains dependent on the location. More ground stations in a specific neighborhood results in a more accurate model. In the past, mainly locations around the equator suffered from a lack of available reference stations. The resulting root mean square error from the inaccuracy of the GIM model on the position is according to Raul Orus Perez [12]:126 cm horizontal and 243 cm vertical in 2014 on a global basis of 30 million single position solutions. Raul Orus Perez [12] indicates that approximately 85 % of the total Ionospheric error can be compensated by the GIM model. This means that the error of 1 to 15 meters can be reduced to 15 to 225 cm.

In order to see the effect of the ionospheric model in this research work, a second ionospheric model is considered : JPL's (only) global TEC-map. This is a map based on more than 100 real time Global Differential Global Positioning System (GDGPS) tracking sites. These provide a real time update every 5 minutes with 5 by 5 degrees resolution. The integrated electron density data along each receiver GPS satellite link is processed through a Kalman filter in a sun-fixed frame to produce global gridded maps of TEC [13][14]. There are also several local maps available that provide either a higher spatial resolution and/or temporal resolution. These maps however have a use limited to certain areas of the Earth with a high density of reference ground stations. These can thus not be used for global applications of ISRO nano satellites and are not used in this research.

This model based approach is most frequently used for single frequency receivers and mostly applied in the post-processing process, in other words, there is no correction on the real time solution. Some high end receivers are update hourly with the newest ionospheric model data and can use those internally to calculate a real time solution corrected for ionospheric errors.

The multi frequency receiver approach uses the difference in propagation delay experienced by the different frequency signals to estimate the total ionospheric error. The main advantage of this method is that it is immediate and localized to where it is applied. It gives an estimate of the ionospheric delay experienced by the tracked signals. One of the remaining sources of error for this multi frequency approach to the ionospheric error mitigation is the previously mentioned receiver analogue frequency dependent error. As the frequency dependent error applies 2 times in an unrelated fashion to both frequency bands used in a dual frequency receiver, its effect is the multiplication of both errors magnitude compared to a single frequency situation. Given that a dual frequency receiver allows for a smaller positioning error margin, the contribution of this error is quite large. To reduce the effect this error is modeled and compensated by the manufacturer in COTS receivers, instead of accurately measured in lab conditions before compensation.

Tropospheric errors are corrected with the help of models. These tropospheric models are being distributed by different weather services, for instance the European Centre for Medium-Range Weather Forecasts (ECMWF). While an IGS solution is also available, the model from ECMWF will be used in this work. The model consist of 2 mayor components: a dry component and a wet component. The dry component is responsible for the majority of the error, ranging from 2,3 meter for a signal coming in at Zenith to 10 meter for a signal just above the horizon.[2] The wet component is significantly smaller. It only contributes a few dozens of centimetres, but it is vastly more difficult to model. The dry component delay is caused by dry gasses whose effects depend on local temperature and atmospheric pressure. Variations of those temperatures and pressures vary relatively slowly, less than 1 % per hour in general, and in

a predictable way. The wet component varies much faster and more local as clouds are a major influence.

The ECMWF model is capable of removing about 95 % of the error when applied during post processing.[2] The remaining 5 % is very difficult to reduce. The further the signal travels through the troposphere, the bigger this error will be. Since water vapor tends to reflect GNSS signals it is generally advisable to reject signals with a view angle below 10 degrees on Earth since both signal strength and quality will be low.
Since the troposphere is not ionized it is electrically neutral, the different frequency signals are affected in the same way. This makes that a multi-frequency approach does not work to mitigate the errors caused by the troposphere.

1.3.4 Error mitigation for the position error

Despite that above multiple mitigation methods are described to reduce the individual error sources, a significant overall error remains if the position determination would be done with the minimum of 4 satellites and one antenna-receiver combination. By using much more satellites it is possible to average out multiple error sources. This will also reduce the effect of the dilution of precision. Therefore we will first discuss the effect of using multiple satellites from multiple GNSS systems. Then we will also consider the effect of using multiple antenna's and/or receivers.

1.3.4.1 Error mitigation by using multiple satellites from multiple GNSS protocols

Combining multiple GNSS systems can be beneficial if increased performance is required. The benefits of additional available satellites and their corresponding signals can be classified in terms of continuity, accuracy, efficiency, availability and reliability.[15]

Improved continuity can be obtained due to the in-dependency of the various GNSS systems. There is a possibility that a single system has a global malfunction. Furthermore, GNSS signals are vulnerable to interference and jamming. This is indeed the reason why nations design and operate their own system to insure independence of other parties. In times of war or heightened tensions, non-military users may be denied from high precision signals. Hence the increased number of signals and frequencies ensures an overall higher continuity and probability of success.

Another benefit is the increased accuracy obtainable with multiple GNSS signals. The increased number of available satellites means that a certain level of accuracy can be achieved in a shorter time-span. This mainly influences the Time To the First position Fix (TTFF), also called the cold start.

The additional set of signals implies that more measurements can be processed by the receivers positioning algorithm. The accuracy of the position determination will be less subject to the influence of satellite geometry as the Positional Dilution of Precision (PDOP) will be small and constant. Another benefit of combining multiple GNSS signals is the possibility to mitigate effects as multipath and interference. This can be achieved by the implementation of signal selection algorithms, ensuring that only measurements of high quality are processed. This allows one to select a high elevation angle cut-off.

The availability of additional satellites also improves efficiency, especially for carrier phase based positioning. The additional satellites will significantly reduce the required time to resolve ambiguities. Another advantage of using multiple GNSS systems is the improved reliability. The additional set(s) of measurements increases redundancy which can be helpful to identify outliers. Disadvantages of the additional use of GNSS signals are the increased power consumption and data generation. The data rate will increase by the integer number of additional GNSS signals used.

Quantitatively, experiments have shown that the addition of GLObal NAvigation Satellite System (GLONASS) measurements improves geometry (PDOP) and visibility by more than 30% and 60% respectively. These numbers are however deduced using a terrestrial placed receiver. The additional GNSS

signals will primarily be beneficial in cases where the receiver is obscured from view and were fast convergence is required. As one is mainly interested in the accuracy achieved in post processing using kinematic Precise Orbit Determination (POD), fast convergence is not required. Although the faster convergence rate is not beneficial, using multiple GNSS protocols is still beneficial to achieve a higher accuracy with higher reliability ensuring a overall more robust solution.

1.3.4.2 Error mitigation by using multiple antenna's and/or receivers

Multiple receiver systems is a setup that is often used in geoscience applications, either in the form of 2 or more independent receivers in the field or by combining ground stations and independent receivers. Its main advantages are for the calculation of relative distances between different receivers that are relatively close together (order of a few tens of kilometers). This is an application we are not really interested in, in the frame of this work.

There are also some applications for the absolute position. It can be used for the reduction of random errors induced by the receiver.

Multiple antennas in combination with 1 receiver might be an option to increase the field of view. This could be particularly an option for certain satellite designs where the antenna might be influenced by obstruction. However, we will not investigate this further as it is not applicable to the satellite system in the scope of this work.

1.4 Past missions and research efforts

Although GNSS was developed for earth based positioning and navigation, the space community started experimenting with spaceborne receivers very early in the deployment of the GPS network. The first spaceborne GNSS receiver was deployed in Landsat 4 in July 16th 1982, figure 1.2. The space environment present different challenges compared to the terrestrial environment. We cannot assume that a receiver working flawlessly on the ground will work properly in space [16].

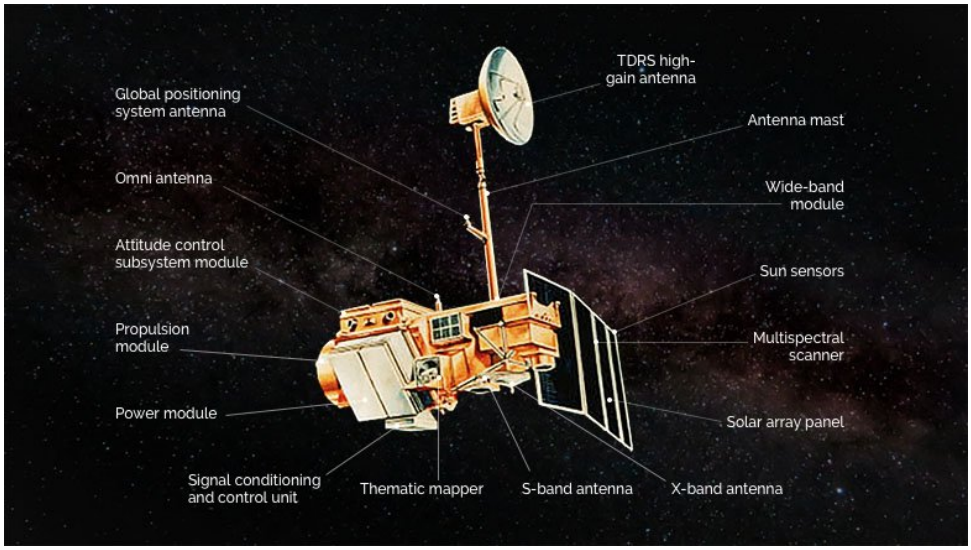

Figure 1.2: the Landsat satellite [17]

There are several problems unique to space born GNSS. This made specialized space based GNSS receivers a necessity in the beginning. The early GNSS receivers were custom equipped to survive the

rigors of the launch, the temperature extremes of space, operation in a vacuum and the increased radiation from the sun.
On top of the previously mentioned mechanical difficulties, one of the most demanding problems faced by all GNSS receivers in space, is the relative large velocity compared to GNSS receiver applications on earth, which results in a larger Doppler shift. As a consequence, a larger band of frequencies needs to be scanned. This is mainly a problem for initially acquiring position lock from an unknown location; the so called 'cold start'. Once a velocity is estimated, the expected Doppler shift can be calculated.

An additional problem, caused by the large velocity of satellites, is that they appear and disappear faster from the field of view. This is especially relevant for those that are positioned low on the horizon of the scanned hemisphere. These satellites may disappear from the observations before sufficient measurement time is available to determine their position accurately. This problem limits the amount of useful satellites for the calculation.

Due to these challenges, for the first 25 years, spaceborne GNSS receivers were purpose-built and very expensive. More recently, smaller satellites have started to use Commercial Of The Shelve (COTS) GNSS receivers for navigational purposes. This developed into the idea to base scientific research on COTS GNSS receiver data. Several studies and missions have already looked into the matter.

A second reason why the interest in COTS recievers has peaked, is the large number of small satellites in space nowadays and in the near future. An industry market report, by the Global Aerospace and Defense Research Team at Frost and Sullivan, estimates that more than 30 commercial small satellite operators are planning to launch up to 4,425 satellites over the next three to five years [18]. To put this in perspective, before 2014 the total number of commercial nano-satellites successfully launched, was less then 100. This means that the market for small satellites is growing at an exponential speed. The market report states that there are multiple new commercial applications, such as traffic tracking, fire detection, crop control etc. This entails also a range of new scientific opportunities. A cheap GNSS receiver with adequate precision could provided the opportunity to get near continues global coverage, for for instance measuring a more detailed gravitation model in space and time. It could be installed, for example, as a secondary payload instrument on several of these commercial satellites.

While the commercial and scientific demand for COTS receivers is clear, it remains an engineering challenge to bring them to wide spread use. Spaceborne devices have very strict constraints with regard to size, shape, weight, power consumption and overall robustness to the space environment. This has been increasingly challenging in the context of size reduction of satellites which led to Cubesats. Spaceborne GNSS receivers should be as small and light as possible and should have a reduced power consumption. Shape constraints might be different from mission to mission and the receiver should be robust enough to survive the vibration load on liftoff and eventual re-entry. The receivers electronic components should also be able to cope with the radiation and vacuum conditions in space.

This chapter will discuss some historic efforts in the area of COTS receivers. For example, at the Delft University of Technology in particular, a Design Synthesis Exercise (DSE) has been treating the subject of a space borne dual frequency GNSS receiver for gravitational research as explained below. In the framework of the Canadian Advanced Nanospace eXperiment (CANX) cubesat project, a collaboration between the European and the Canadian Space Agency, in flight testing of a COTS dual frequency GNSS receiver has been performed and this will also be discussed.

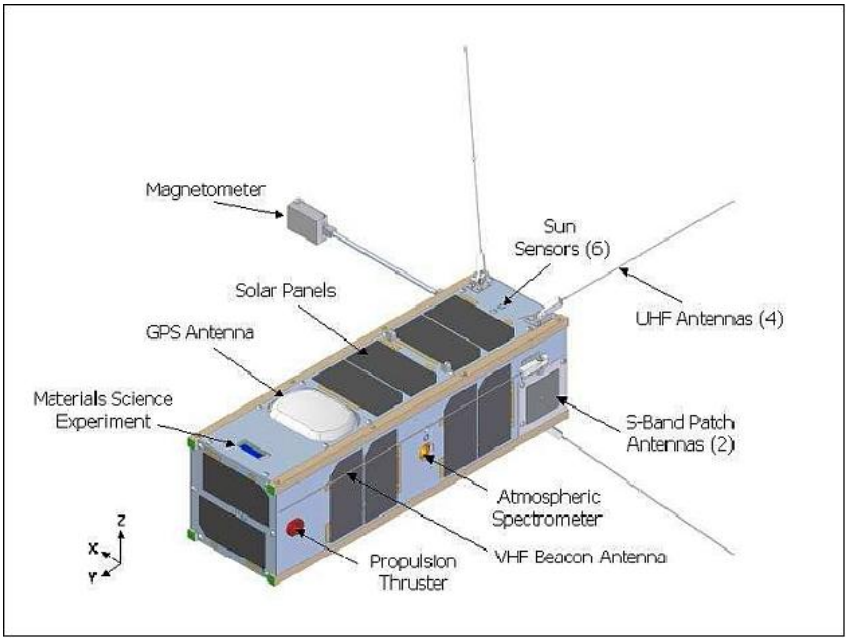

Figure 1.3: Overview of the CanX-2 bus and device locations [21]

1.4.1 Past missions with COTS GNSS receivers on Cubesats

At the turn of the millennium, the interest in using COTS receivers started to rise. Experiments to facilitate the use of such receivers where conducted. The Belgium company Septentrio, in collaboration with DLR, did extensive tests on one of their dual frequency receivers: the PolaRx2 [19]. The test exposed the receiver to similar circumstances as it might experience in space. The experiments included vibration testing and exposure to radiation[19]. Position measurement performance tests where also performed. Unfortunately, no tests were performed with a setup that resembled an actual configuration of the receiver and the antenna in a way that could be mounted on a satellite.

The unrealistic testing setup, was probably a key reason for the difficulties experienced on one of the first missions to fly a COTS receiver, CANX-2, as will be explained below.

The Canadian satellite CANX-2 was a pioneering mission in the field. This nano satellite was the first to successfully deliver GPS navigation fixes and raw measurements, meaning the data on which the receiver bases its internal position calculations, with a COTS GPS receiver, NovAtel OEM4-G2L, in April 2008 [20]. These raw measurements are a requirement for useful scientific applications, as explained in the chapter on error mitigation 1.3.

However, the CANX-2 mission suffered major problems with its GPS position fixes, mainly due to a worse than expected signal to noise ratio at the receiver. The value was up to 10 dB lower during the mission than during the pre-mission test. This leads to a reduced number of satellites that can be tracked by the receiver and consequently worse position calculations [20].

One of the major factors leading to this poor signal to noise ratio was the antenna configuration as stated in the article [20]. The antenna was placed in a recessed area of the satellite bus, meaning it was located more inward then the face panel, in order to fit in the launch pod. This resulted in an antenna that was only partially above the satellite bus face panel and without ground plane, as can be seen figure 1.3. Although care was taken that the antenna patch was level with or above the panel in order to reduce the likelihood of altering the antenna gain pattern, it is assumed that this raised problems, as can be noticed upon inspection of figure 1.3.

This experience leads to a series of tests in this work where the effects of a ground plane will be investigated. Lack of a ground plane can lead to effects as seen in figure 1.4 below [22].

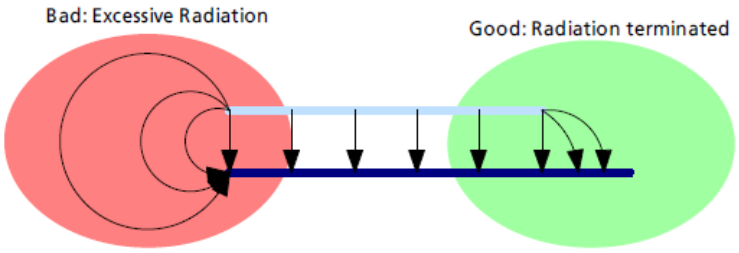

Figure 1.4: The dark blue groundplane is not extending beyond the light blue antenna on the left side, causing a bad radiation pattern on the antenna edge. The extension of the ground plane on the right enables the right antenna edge to terminate radiation on the ground plane [22].

Figure 1.4 shows the disturbance of the patch radiation antenna pattern when there is no groundplane sufficiently exceeding the antenna boundaries. Such disturbance will lead to a shift in the antenna phase center and radiation pattern.

After the successful test with the NovAtel OEM4-G2L receiver in the CANX-2 mission, it was used in multiple other missions such as CANX-4, CANX-5 and JC2Sat-FF.

The CanX-4 and 5 satellites were developed at the University of Toronto to execute a demonstration mission testing Satellite Formation Flying. This was done using a GNSS receiver with high-accuracy tracking algorithms for autonomous formation flying in the presence of orbital perturbations. The CanX program was, similar to TU-Delft's DelFI programme, designed to allow students to gain experience in the development, manufacturing and operation of satellite missions. CanX-4 and 5 demonstrated a carrier-differential GPS measurement technique for high-precision relative position determination, and a nano-satellite propulsion system for use to maintain the formation[23].

In these CANX-4 and 5 missions the GNSS receiver was mainly used for relative navigation. Relative navigation means the navigation between satellites flying in formation. A relative positioning accuracy of less then 10 cm was achieved [23]. This is a less demanding task than absolute position fixing for scientific purposes as intended in the context of this study. In essence, by using multiple satellites one is using differencing as described in the chapter on error mitigation as primary error mitigation approach which disregards the majority of all other errors in the relative position measurement. In the context of providing sufficient accuracy for scientific applications the CANX missions did not yet reach success.

The large velocity problem mentioned above in the introduction was especially relevant for COTS receivers that are made for large scale applications on earth. They are not able to propagate orbital dynamics risking significant drifts in velocity estimations which might result in a bad estimate of the Doppler shifts and consequently push the receiver to analyze wrong frequency bands. This results in the CANX-2 mission in a drop of all tracking signals and triggers a cold restart. Since the cold starts require a significant amount of time this results in significant gaps in the observations.

A GNSS receiver has several tracking channels. These channels are meant for searching and tracking of GNSS satellites. Each channel searches in a dedicated set of frequencies by sampling and once a satellite has been detected, a dedicated channel is assigned to that satellite to continuously track it. For example the NovAtel OEM4-G2L receiver has 24 channels. [24]. When tracking of a satellite with 2 frequencies is required, 2 channels need to be used for 1 Satellite as each frequency needs its channel [25]. Doppler shift will require that the frequency of the channel during the tracking process needs to be adapted as a function of the changing relative velocity.

A first approach to solve the problems, caused by Doppler effect, is to use the receivers full tracking capability by searching as many GNSS satellites as possible : GPS, GLONASS, GALILEO. This method

will require tracking satellites in a different frequency band for each satellite constellation. The advantage of the method is that the opportunity to quickly find satellites is large, but there are multiple disadvantages: A first one is that by using multiple GNSS constellations there is no guarantee that the satellites positions selected in the limited amount of channels will have a good spread over the hemisphere. This may lead to a worse geometric dilution of precision as explained in the figure 1.1 .

A second major disadvantage is that all the different GNSS systems have different internal errors which are difficult to estimate, if not enough good quality satellites from the same system are tracked. A third potential disadvantage is that many of the selected satellites might be on the edge of the detection hemisphere and consequently that their signals are of low quality and rapidly lost due to the relative movement of the satellites. This could also result in a cold restart because for every satellite tracked one channel is unavailable to search for another one. One of the methods to deal with these disadvantages is to increase the number of channels, but this also increases the required computing power and energy consumption in the receiver. It also becomes clear from the above that for a receiver with a limited amount of channels, an alternative approach is necessary.

An alternative approach to solve the problems caused by Doppler effect is used by the receiver NovAtel OEM4-G2L. The NovAtel OEM4-G2L only uses the GPS constellation. Using one constellation immediately ensures a good position spread of the satellites, avoiding geometric dilution of precision. It also limits the amount of frequencies that has to be scanned. In order to speed up the scanning process once a position lock is obtained an additional software program provides a better estimation of the Doppler shift over time. In addition, the number of simultaneously tracked satellites is limited to the 6 signals with the highest signal to noise ratio, leaving more channels open for finding even better alternative satellites. Also, a method to avoid cold starting was developed by the university of Calgary [20]. In this method the receiver was only started at specific times where a predetermined GPS configuration was stored in memory. This allowed a fast warm restart at regular time intervals.

In the case of the CANX project, the problem was tackled in a rather brute force approach. The new satellite in the line was the CASSIOPE (CAScade SmallSat and IOnospheric Polar Explorer). This satellite still uses NovAtel OEM4-G2L receivers, but this time not just 1, but 5. Of these receivers, 4 are combined with independent patch antennas on the zenith facing panel of the CASSIOPE spacecraft [26]. The fifth one is connected to a NovAtel pinwheel antenna with an anti-velocity pointing boresight direction to collect high-rate ionospheric radio occultation (RO) measurements[26]. Due to the larger antennas used in the later CANX projects, acquisition of the signal was a problem of the past. The new multiple receiver setup allows for far more options; with the help of differentiating multiple antenna receiver combinations the attitude of the spacecraft can be determined, the different antenna errors can be reduced. The fact that for the first time an attitude could be calculated opens a whole new range of both calibration options as well as a way to verify the results. This allows that the positions obtained by the GPS receivers can be compared with other instruments such as a star-tracker. With this comparison, it could be proven that with star sensor-based yaw, pitch, and roll angles, a precision of 0.1 degrees to 0.3 degrees, for filtered GPS-based attitude angles, is demonstrated. This precision is reached after calibration of differential phase patterns for individual antenna pairs. Not surprisingly, with this data intensive setup, the actual constraint for precise orbit determination became the computing power and data down-link capacity, since this has to be shared with other instruments. The capacity constraints enforce daily gaps of 5 to 7 hours in the data availability. Even with these gaps, the orbit determination within a box of 1 meter was possible for 80 percent of the days in orbit so far[26]. With full data availability, sub 10 cm position determination is possible. Theoretically all the way down to 8-5 mm position accuracy is possible. However, the satellite lacks retro laser reflectors to verify this accuracy.

Although for none of the above missions, center of mass knowledge has been discussed, it is important to know it accurately for scientific results. For most scientific purposes the movement of the center of mass is the reference point on the satellite. All positions are calculated by the receiver with respect to the antenna phase center. This position should be recalculated to the center of mass of the satellite. This center of mass position might slightly change over the mission, for instance, when mass is being ejected. In addition, a good positional awareness of the antenna phase centre relative to the mass centre is important. This implies that attitude knowledge is an important factor. Since for scientific purposes

we are actually interested in the position of the mass centre and not the antenna phase centre where the receiver calculates the position.

Finally, attitude control of the cubesat satellite plays an important role in the GNSS receiver tracking capabilities. It is very important to have a satellite that is stable along its 3 axis. Rotation or other movements along one or more of the axis constantly changes the field of view of the antenna. It is obvious that this complicates the tracking seriously as was already clearly stated in [20]. This lack of attitude was also a major issue in a previous mission of the Indian Space Agency, INS-1B, which resulted in a failure to get position fixes.

1.4.2 Past work at the University of Delft.

The aim of the previously mentioned DSE project was to design a cubesat with as specific purpose to fly a dual frequency GNSS receiver to research the earth gravity fields. The report of this project was : *Gravity Explorer Satellite (GES), Providing data on temporal changes in Earth's gravity field for scientific use at low cost.* [10] In this project, the GNSS receiver was the primary payload for which the entire design was optimized. This provided a degree of design freedom that will not be available in the satellite for which this study is being done, INS-1D and which has other primary objectives.

The research done in the DSE framework was entirely theoretical, but it demonstrated the conceptual possibility to equip a cubesat with a COTS receiver. The study looked into several receiver alternatives from Septentrio and NovAtel. The selected receivers from the DSE study were not available for this study as will be explained in the chapter on Receiver Selection 3. The aim of the receiver selection was to find a receiver with a limited measurement noise that enabled a positioning accuracy after processing of less than 1 cm. Since all the receivers reviewed in the DSE project met this requirement, the final trade-off in the selection was made on practical concerns such as power consumption and weight. On this basis the model AsteRx-m OEM from Septentrio was selected. The capabilities of this receiver were never tested in the frame of the DSE project. Obviously, the choice of the Antenna that was combined with the receiver was also a major consideration. Given the earlier mentioned design freedom a relatively large antenna could be chosen. The design considerations revealed that the optimal placement of the antenna would be on a surface of the satellite providing a ground plane as large as possible and with a minimum amount of obstructions. The finally selected antenna was model ACCG5Ant-2AT1 from Antcom with a diameter of 67 mm which is larger than the space we will have available on an INS-satellite in this project.

The signal to noise ratio for this system was theoretically calculated for the relevant frequencies in this research context. For L1 GPS the value was 48 dB in passive tracking mode and 76 dB in active tracking mode. For L1 GLONAS the calculation result was 47 dB in passive and 75 dB in active tracking mode. The active tracking values found in this study were relatively high due to the fact that the LNA gains are added directly as signal gains, which is not reflecting reality as the LNA will also partly amplify the noise.

It is not the aim anymore to really continue the work on this dedicated cubesat concept for gravity field research for cost reasons. The general knowledge obtained in this work can be useful for the adaptation of the INS cubesat program with dual frequency receivers that could achieve the objectives of the gravity field research. In a later work for the course of microsat, different concepts of this same dedicate satellite idea were analyzed. Finally a project, as part of a bachelor minor course, looked into the data rates required for the down-link connection of such a satellite.

The current study will complement the theoretical results of the past theoretical works with test observations.

1.5 ISRO Nano Satellites

Indian Space Research Organization (ISRO) Nano Satellites or INS is a versatile and modular Nano satellite bus system envisioned for future science and experimental payloads, see figure 1.6. With a capability to carry up to 3 kg of payload and a total satellite mass of 11 kg [27]. The INS system is developed as a co-passenger satellite to accompany bigger satellites on the Polar Satellite Launch Vehicle (PSLV) [27].

The primary objectives of INS system as defined by ISRO are to 1.6:

- Design and develop a low cost modular Nano satellite
- Provide an opportunity for ISRO technology demonstration payloads
- Provide a standard bus for launching on demand services
- Provide an opportunity to carry innovative payloads for Universities and research laboratories

From these opportunities provided by ISRO, we made use to test COST GNSS receivers for scientific use.
PSLV-C37 carried two ISRO Nano Satellites INS-1A and INS-1B as co-passenger satellites, which was launched on Feb 15, 2017. It was a record breaking launch that deployed 104 satellites1.6.

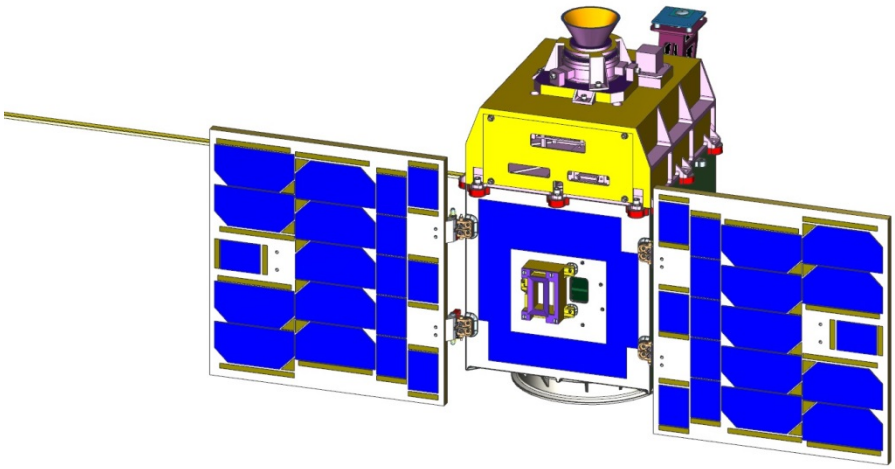

Figure 1.5: INS 1A[28]

1.5.1 INS-1C

INS-1C was launched by PSLV-C40 on feb 12, 2018, as a co-passenger satellite1.6. The satellite was brought into a Sun Synchronised Polar Orbit (SSPO) with the folowing characteristics : a pericentre of 495 km and apocentre of 508 km, and an inclination of 97.56 degrees. The Two-Line Element set (TLE) can be found online [29]. This orbit somewhat limits the scientific applications of the obtained GNSS signals, since the nature of a sun synchronised orbit implies that the sun is always seen under the same angle. For instance, tidal patters are more difficult to correct for in gravitational research.

The INS-1C satellite measures 24.5 by 22.7 by 21.7 centimetres and weighs 11 Kg. The power is provided by two deployable solar arrays and body-mounted solar cells, delivering 27 W of power. This power output is stored in a 11.2 Amp-hour Li-Ion battery and distributed to the various users on the

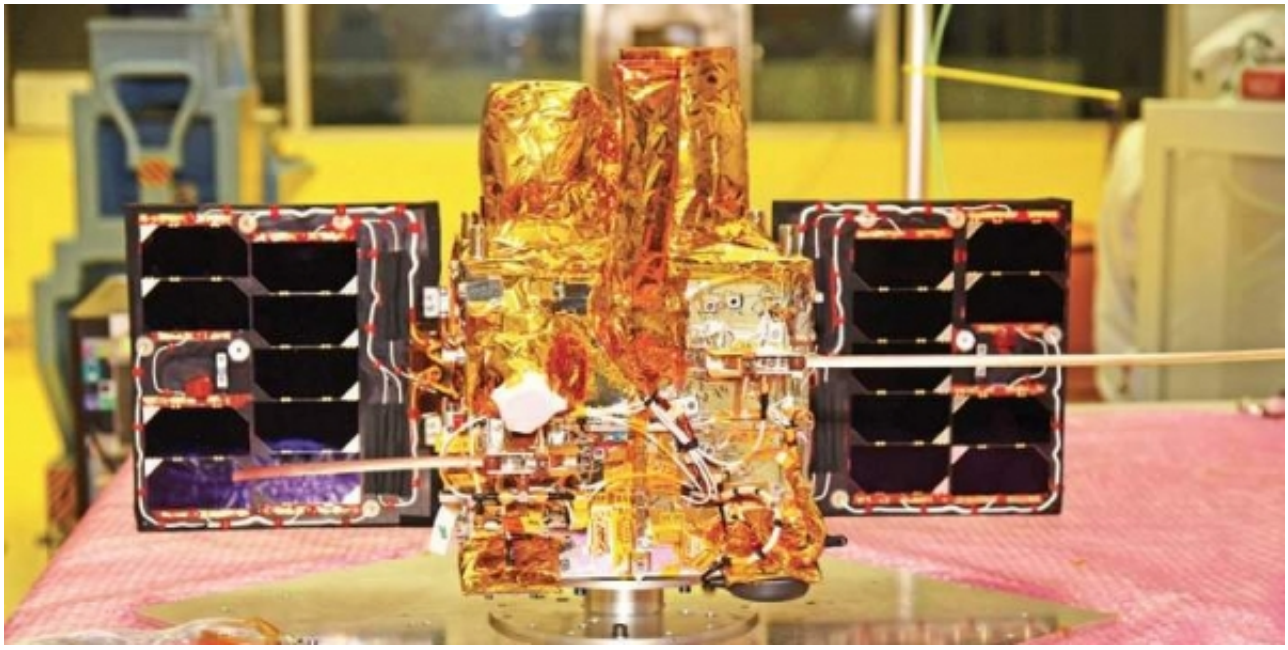

Figure 1.6: INS 1C[27]

satellite. Attitude determination is accomplished through a combination of sensors including a Microelectromechanical system (MEMS), Inertial Measurement Unit (IMU), Micro-Sun Sensors and a three-axis magnetometer. A star tracker provides precise pointing knowledge after initial attitude stabilization. The stabilisation system is provided by a combination of reaction wheels and magnetic torquers with a pointing accuracy better than 0.5° on each axis. This is more than sufficient for satellite tracking with a GNSS receiver and for many Earth-imaging applications which is the main purpose of this mission. The pointing knowledge is even higher at 0.1°, which is important for the mass centre location knowledge.

INS-1C carries a Miniature Multi-spectral Technology Demonstration (MMX-TD) camera as main payload from the Indian Space Applications Centre. Data sent by this camera are useful for topographical mapping, vegetation monitoring, aerosol scattering studies and cloud studies.

It is the third satellite in the Indian Nano Satellite series and it is carrying the Skytraq receiver for the first time with the option to transmit the raw data. The INS platform is equipped with an on-board memory of 8 GB in the form of an SD Card. However, the raw data of the GNSS receiver is separately stored on a dedicated 500 MB memory unit outside the satellite bus, next to the receiver. Payload data playback is available at a data rate of 1Mbps via S-Band while commanding and telemetry exchange is handled in VHF and UHF. INS is rated for an in-orbit life of six months. This is theoretically sufficient for most technology demonstration missions with limited budget.

Unfortunately ISRO lost contact with the satellite early April 2018, less than 2 full months after launch. Given the short lifetime of the satellite, no relevant raw data were ever transmitted. As a consequence, these data were unexpectedly not available for this work.

1.6 Problem statement

GNSS receivers and especially GPS receivers have been used in spaceborn applications for the last four decades [16]. However, most of them, have been purposely built or were limited-series receivers. This makes them extremely expensive, for example Blackjack and IGOR [30] which cost more then 1 million

dollar [30]. Over the last several years, with the breakthrough of nano satellites, specifically cubesats, commercial of the shelf (COTS) GNSS receivers have made their way into space several times [20][23]. These receivers have been flown primarily as either technology demonstrations or as a navigational aide. In this report we will try to see if there is a potential to use these receivers for scientific purposes as well, in the frame of a collaboration between TU-Delft and the Indian Space Research Organisation (ISRO).

More specifically, ISRO has started a program with a series of nano satellites on which they do technology demonstrations. PhD Student, Sujay Narayana, working at TU-Delft, is directly involved in the ISRO project to design and operate future ISRO nano satellite missions, with a focus on signal processing and GNSS receiver modules as payload on these satellites. It is the longer term aim to equip the future nano satellites with dual frequency receivers to enable their use for a variety of scientific applications, such as: Earth gravity field research, Ionospheric research and Thermospheric research. These require centimetre level position accuracy measurements.

In this work we will analyze and test conditions to reach this scientific goal. This will be done by testing a selected receiver, in this case a single frequency receiver from Skytraq that is used on the nano satellite INS-1C from the Indian Space Research Organisation launched in January 2018[27]. The study will aim to determine as closely as possible the capability of this receiver on Earth as a reference framework to test a future dual frequency receiver. As the receiver forms a system with the antenna, it is also important to take a closer look at the antenna used on the INS-1D satellite and its mounting conditions. Therefore, we will have a look at the antenna placement and potential antenna alternatives for future missions.

Given that the tests happen on Earth we should assess the potential errors and failures that the conditions in space might introduce. It is both important to look at potential problems that the circumstances on earth might induce, such as the tropospheric errors, as well as the typical circumstances in space, such as radiation ionization. In a test program we will define relevant tests to assess the accuracy of the Skytraq receiver and the antenna by comparing to results from a reference receiver and antenna available at TU-Delft.

We not only want to get an impression if the position information that can be obtained from the single-frequency Skytraq receiver is sufficient to calculate the trajectory of the satellite. We would also like to find out if the receiver is accurate enough to detect perturbations in the gravity field, which can be important for certain scientific applications such as gravitational field analysis, atmospheric density models and space weather. Given the limitations of a typical single frequency receiver, the ambition will be limited to assessing whether a sufficient accuracy can be obtained so detecting some variations is feasible. If this is the case it makes sense to follow-up with testing the capabilities of a future, space-grade, dual frequency receivers of the same series and manufacturer. Those tests can than later be compared to the tests of this report.

It is the aim to continue this work with a broader research project at TU-Delft to complement very expensive scientific satellites with arrays of less expensive, and less accurate, nano-satellites that combined can be used to obtain relevant information at a much lower mission cost.

We aim to answer the following research questions in this work :
Can relevant scientific information be derived from GPS measurements on a cubesat?

- What position accuracy of the current single-frequency Antenna-Skytraq receiver as used on the INS-1C nano satellite can be obtained on Earth and what factors influence the position accuracy?
- What position accuracy can be achieved in an in space simulation of the Receiver System?
- What conclusions and design recommendations can be derived from the tests executed to answer the questions above, to improve the performance of COTS receivers on future missions?

2 Data Format and Data Analysis Software

In this chapter we describe the data format and different software packages that will be used to analyse the receiver data and to make position calculations.

2.1 RINEX

The Receiver Independent Exchange Format (RINEX) in full, is well described by its full name. It is an independent data format for raw satellite navigation data and the format used in this work for data post processing. There are a few different version of the RINEX format available. The one used in this study is RINEX 2.11. RINEX version 2.11 is a de-facto standard for storing all the data needed for all kinds of GNSS positioning and navigation. This standard provides means to efficiently store data transmitted from GPS, GLONASS, GALILEO and geosynchronous satellite (GEO)/Satellite-Based Augmentation Systems (SBAS) satellites, as well as meteorological data and the fundamental observations made by GNSS receivers (code, phase, Doppler and time)[31]. RINEX versatility and extensive documentation has made it the data standard of choice for data input in most post processing software's, both in real-world practical application as in research and development projects.

The format consists of seven ASCII file types[31]:

1. Observation Data File
2. Navigation Message File
3. Meteorological Data File
4. GLONASS Navigation Message File
5. GEO Navigation Message File
6. Satellite and Receiver Clock Date File
7. SBAS Broadcast Data File

The scope of this report is the Observation Data File. This file allows to store the most important data collected by GNSS receivers, including all the observations needed for GNSS positioning and navigation. The other files are either not provided by the receiver or already incorporated in the used software.

RINEX 2.11 is chosen above the more recent 3.XX versions because there is larger expertise with it and it is supported by a larger number of software packets. On top previously mentioned arguments, the added capabilities from the RINEX 3.xx versions like the support off L5 frequencies are useless for this study because they are not supported by the receiver. It is important for this study that RINEX 2.11 supports the measurements of pseudo-range, carrier-phase and Doppler systems for GPS, GLONASS, Galileo and Chinese satellite navigation system Beidou.

2.2 VENUS GNSS vieuwer

Skyyraq VENUS GNSS Viewer 8 is an interface for real-time monitoring of GNSS signals. The viewer allows for a graphical representation in real time of the incoming signals. It indicates the time until the TTFF. It shows when a signal is first acquired. This is shown by an empty bar with the satellite number indicated below it as shown in figure 2.1. After the ephemeris data is collected and the satellite signal is used for position fixing, the signal bar will turn into a solid bar.

Satellites GPS/GLONASS/Beidou/Galileo are displayed in Earth View below it as can be seen in figure 2.1. This graphical representation gives a first impression of the spread of the satellites. Together

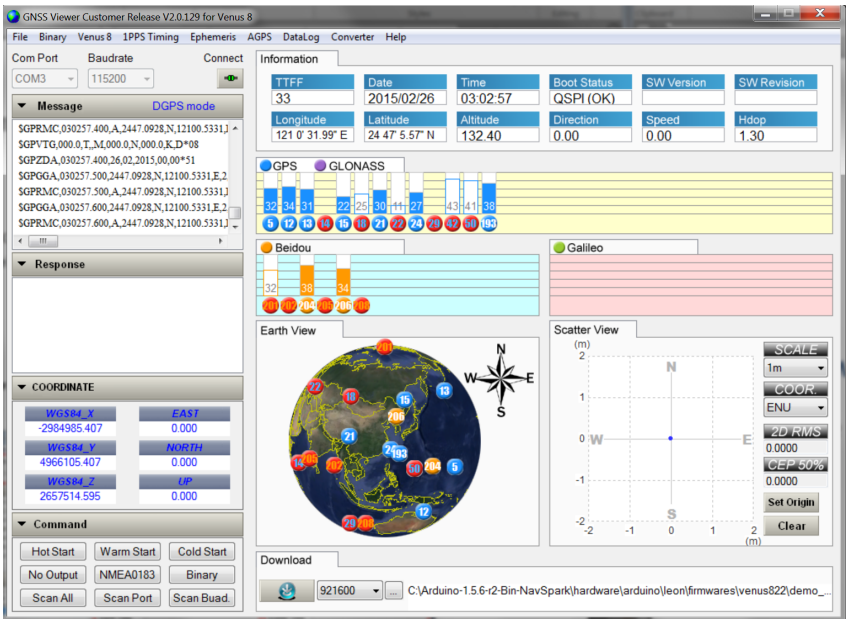

Figure 2.1: VENUS GNSS Viewer 8, a screen shot [32]

with the Scatter Diagram on the bottom right of the graphical interface it gives a preliminary indication of the quality of the data. The program is used for the recording of the receiver output data in the Skytraq native format. The graphical interface was the reason for which it was selected above a pure log-program.

2.3 RTKLIB

RTKLIB is an open source processing program used for standard and precise positioning calculations with GNSS [33]. RTKLIB itself is a portable program library, this library is then used by several open source APs (application programs) that are available for free[33].

The actual position calculations of this package are not used in this study, we rely on GIPSY for this. What we did use of this package is its conversion algorithm, data converter RTKCONV. It is a raw Skytraq receiver data to RINEX conversion program. This only works when using the receivers standard output data format as set by the manufacturer, in this case Skytraq. RTKCONV can't be used to process the actual mission data. For the actual testing where the data are in the format extracted from Venus 8, there are no downlink problems requiring special condensed formats, and RTKLIB can be used.

RTKPLOT will be used to analyze the position data that will be calculated in the Skytraq receiver itself during some of the tests.

2.4 teqc

Teqc is a program designed to solve many preprocessing problems with GPS, GLONASS, Galileo, SBAS, Beidou, Quasi-Zenith Satellite System (QZSS) and Indian Regional Navigation Satellite System (IRNSS) data, especially in RINEX or BINary EXchange (BINEX) format. Teqc (translation, editing, quality check) gets its name from its 3 basic functions[34]

- Translation: binary data reading/translation of native binary formats from different GNSS receiver types
- Editing: including time windowing, file splicing or other filtering, metadata extraction, editing and or correction of RINEX header metadata or BINEX header metadata records
- Quality Check: Quality checking of GPS and/or GLONASS data

The teqc program is freeware that is maintained by the UNAVCO community. Teqc has enabled the analysis of the three basic kinds of RINEX formats that are used throughout this report :

- OBS for the RINEX observation data file,
- NAV for the RINEX navigation message file,
- MET for the RINEX meteorological data file.

The last one will only be produced by the verification receiver for which we use a LEICA SR520 receiver. The most extensive use of teqc in this work is related to the quality check and filtering of the data used in each of the different tests described in chapter 5. Teqc currently handles RINEX version 1 and 2.

2.5 GIPSY(X)

It was previously mentioned that this study opts for GIPSY as post processing tool. We will use GIPSY in this thesis trough a tool provided by Geoscience Australia. GIPSY or GIPSY-X is the GNSS-Inferred Positioning System and Orbit Analysis Simulation Software package, the multiple navigation systems variant of the old GIPSY-GPS. GIPSY is developed by the Jet Propulsion Laboratory (JPL), and maintained by the Near Earth Tracking Applications and Systems groups. It builds on more than 25 years of JPL experience with GPS data analysis. The original GIPSY-OASIS version was written in Fortran and limited to the Global Positioning System (GPS). The new generation GIPSYX, written in C++ for Linux , is capable of analyzing data from the following GNSS systems: GPS, the Russian GLONASS, Galileo and BeiDou. It can read correction data from the following systems and technics: the French DORIS system, the Satellite Laser Ranging (SLR) system and Doppler tracking. The software is used by hundreds of researchers for academic purposes and is freely available at the TU-Delft.

GIPSY is used for the precise orbit determination of Low-Earth orbiters such as Jason-1, Jason-2/OSTM, GRACE, Space Shuttles and many other satellites. It is also well suited for CubeSat's that are relevant to this study and the major research subject : the INS satellites.

GIPSY has many users that apply it in terrestrial positioning for geophysical research topics : Earth deformation, plate tectonics, Ice flow, climate studies through observation of the troposphere and ionosphere. It is also used for reference frame with respect to geocenter and scale and Earth rotation parameters. Finally GIPSY can also be used for Airplane positioning.

3 COTS GNSS Receivers

Recent scientific applications of spaceborn GNSS have relied on dedicated receivers such as Blackjack, GNSS Receiver for Atmospheric Sounding (GRAS) and Lagrange. These receivers can all be characterized by a high level of specialization, limited production volumes and demanding qualification programs, resulting in a price tag in the order of millions of dollars. This situation causes an increased interest in affordable alternatives for missions where ultimate reliability and space qualification are not required. Research has shown that COTS geodetic GNSS receivers can, with little to no modifications, operate with the increased signal dynamics and environmental conditions of a LEO.

In this chapter we will first discuss the key conditions to be taken into account for COTS GNSS receivers in space. We will then elaborate on different receiver types and the adjustment that needs to be made to these receivers for operation in space. We will finally discuss the selection used in ISRO INS nano satellites and in this work.

3.1 Ionizing radiation

The key environmental difference between space and Earth's surface is the substantial presence of cosmic radiation in space. This radiation has a large influence on the lifetime of the GNSS receiver, by accelerated degradation of the internal and external components. Most COTS receivers are not designed to operate in a high radiation environment, so in order to use them for space applications this has to be taken in account. The critical factor is the Total Ionizing Dose (TID) which is depend on the orbit height. This is also the factor where testing is mainly focused on. The TID takes into account the total cumulated radiation over the receiver's lifetime in orbit. Apart from the accumulated radiation, the extreme peaks in radiation levels can cause problems. Since the satellite will be in LEO, Earth's magnetic field will limit the peak radiations to an acceptable level, so they will not cause additional problems. [24][19]

TID testing of IGOR, a commercial version of BlackJack, has determined a maximum TID of 12 *krad* before IGOR fails. A TID of 12 *krad* is enough for a lifetime of several years in LEO.

TID test on COTS receivers such as OEM4-G2 and PolaRx2 have resulted in lower TID values 6 *krad* and 9 *krad*. [24] [19] The max TID of 6 krad of OEM4-G2 results already in a life time of at least 2 years in LEO. [30] In addition we know that the Skytraq receiver on board of the INS-1B mission has been working for almost 9 months now, without a hitch. This indicates that it is able to cope with TID for at least 9 months. We aim for a lifetime of 3 years. For TID's of reference single- and dual-frequency GNSS receivers, the reader is referred to tables A.1 and A.2 in appendix A.

3.2 Other environmental conditions

The presence of cosmic radiation is not the only environmental difference compared to the conditions on Earth. There is also the near vacuum condition in the upper atmosphere, but this has no impact as long as there are no air-pockets in the receiver. More important is the extreme temperature variation

experienced by an object in space. The receivers operating temperature range is limited, it is therefore important that the satellite provides sufficient thermal control. This also means that the heat generated by the receiver itself should be taken into account.

3.3 Dual- and single-frequency GNSS receivers

Dual-frequency GNSS signal reception is generally known as the tool of choice for Precise Point Positioning (PPP) over the single-frequency alternative. The dual-frequency receiver is capable of receiving GNSS signals on two frequency bands from the same satellite. The typical dual-frequency receiver operates on both the L1 and L2 frequency bands, which enables the mitigation of ionospheric delays. When compared to the single-frequency alternative (L1 only), the dual-frequency option is technically more complex and therefore more expensive. To examine what the advantages of a dual-frequency receiver are for the improvement of positioning accuracy in future INS missions, an evaluation on both receiver types is necessary. This section provides a basic elaboration on dual-frequency and single-frequency PPP, a description of reference GNSS receivers, and a discussion on the differentiation with multiple GNSS receivers.

3.3.1 Dual-frequency GNSS receiver

In PPP ionospheric delays are most often handled by means of a dual-frequency GNSS receiver that forms the so-called ionosphere-free linear combination of L1 and L2 carrier phase and pseudo-range observations [35]. Dual-frequency positioning reaches a centimetre-level accuracy, but unfortunately shows slow convergence towards this final result (20-40 minutes). However, the mission does not require accurate real-time positioning so fast convergence of the receiver accuracy is not essential.

Furthermore, the aforementioned ionosphere-free linear combination amplifies multipath and receiver measurement errors and is therefore very noisy. Increasing the pseudo-range will increase this noise.

3.3.2 Single-frequency GNSS receiver

The formation of the ionosphere-free linear combination of L1 and L2 is not possible via single-frequency PPP, since the single-frequency receivers do not operate on both bands. In single-frequency PPP the ionospheric delays can be handled by using a linear combination of L1 code and carrier phase data, or by using external data on ionospheric delays (e.g. from the gridded global ionosphere maps). Single-frequency positioning reaches a decimetre-level accuracy and converges quickly to its best accuracy. But as mentioned earlier, fast convergence is of no importance for this mission.

3.3.3 Comparison of dual-and single-frequency GNSS receivers

Comparing various dual-and single-frequency receivers, it is concluded that the gain in accuracy of dual-frequency far outweighs its loss in affordability, when we considered the COTS version.For any applications that require accurate position knowledge, dual-frequency receivers are the best choice. An overview of the studied receivers, together with their main characteristics, is provided in tables A.1 and A.2 in appendix A.

3.4 Velocity restriction

One modification that is required to use COTS receivers in a space environment is the removal of the Coordinating Committee for Multilateral Export Controls (COCOM). The COCOM limits the operational velocity in order to avoid abuse of those receivers in weapon systems. To ensure operability in

space this limiter has to be removed.

Manufacturers of COTS receivers charge additional cost in the order of US$ 1,000.00 to US$ 7,000.00 for the removal of the COCOM [36]. However although the cost is substantial, here, it is not the main obstacle but rather the willingness of the manufacturer to start the procedure.

3.5 Receiver Selection

The table 3.1, shows seven theoretical dual frequency receiver candidates to fly on future INS missions. All these receivers are from NovAtel or Septentrio, however, both manufacturers were either unable to provide the receivers due to export restrictions or unwilling to go through the procedure to apply for COCOM restriction removal for this project. Here, the COTS nature of the product is actually a disadvantage since the cheap price entails that manufacturers expect to sell a large number of receivers and are not willing to go through considerable expenses for a limited sales amount.

NovAtel has already receivers launched for different Canadian Space Agency projects, but was unwilling to work with another space agency. Septentrio also raised a technical issue on top of the COCOM restriction removal. It was afraid that its band filters were to narrow to deal with the Doppler shift of the GNNS signal.

After it became clear that the preferred manufacturers were unable or unwilling to sell a dual frequency receiver for this project, other companies have been contacted, such as DataGrid and Swift Navigation, but they completely failed to respond.

After these failed attempts to buy dual-frequency receivers, it was decided to go with Skytraq. The ISRO already has a working relationship with the Skytraq company. Skytraq has a dual frequency receiver in its development pipeline. Originally this receiver was meant to be ready by the end of 2017, however the project has been delayed. This receiver is end 2019 not yet commercially available. Because of this, we did not have any access to a dual frequency receiver. This was a major drawback for this work. Also the specifications for this Skytraq receiver in development are not yet made public and could not be included in table 3.1.

An additional consideration is related to the raw data extraction and the transmission of raw data from the satellite to Earth. The good relation between the Skytraq company, ISRO and the research team at TU-Delft, ensures that all the raw data of the receiver are accessible. This is important to post-process more accurate position data as required for scientific use. However the link budget for data transmission from the INS-satellite to Earth is limited. On top, it will have to be shared with other experiments and household data of the satellite. Therefore it is important that the raw data are going to be pre-processed on the satellite in order to filter the most relevant raw data for transmission. The tests later in this work will provide indications for filter-strategies that allow to limit the amount of transmitted raw data.

Ultimately, the Skytraq S1216F8-GL receiver was used in the tests and on INS-1C. This is a single frequency receiver that will be used as a basis for the future dual frequency receiver from Skytraq. It is obvious that the performance of this single frequency receiver is inferior to the dual frequency receivers in table 3.1.

The data sheet of the Skytraq S1216F8-GL receiver can be found in Appendix B.

Receiver label	Rec-1	Rec-2	Rec-3	Rec-4	Rec-5	Rec-6	Rec-7
Manufacturer	Septentrio	Septentrio	Septentrio	NovAtel	NovAtel	NovAtel	NovAtel
Model	AsteRx3	AsteRx-m	AsteRx2e	OEM615	OEM627	OEM625S	OEM628
Frequency channels	L1/L2/L5	L1/L2	L1/L2	L1/L2/L2C	L1/L2/L2C	L1/L2/L2C	L1/L2/L2C/L5
GNSS protocols	GPS/Glonass/Galileo	GPS/Glonass	GPS/Glonass	GPS/Glonass/BeiDou/Galileo	GPS/Glonass/BeiDou/Galileo	GPS/Glonass	GPS/Glonass/BeiDou/Galileo
GPS carrier phase measurement accuracy L1/L2 (mm)	1.0/1.0	1.0/1.0	1.0/1.0	0.5/1.0	0.5/1.0	0.5/1.0	0.5/1.0
Tracking performance (dB - Hz)							
Tracking	26	26	26				
Acquisition	33	33	33				
Maximum data rate (Hz)	100	25	25	50	50	20	100
Mass (g)	60	40	60	24	24	56	37
Length x width x height (mm)	60 x 90	47.5x70x8	60x90	71x47x11	71x46x11	100x60x15.31	100x60x9
Operating Temperature (°C)	-40 - 70	-40 - 85	-40 - 85	-40 - 85	-40 - 85	-40 - 85	-40 - 85
Power consumption (W)	2.9	0.49	1.5	1.0	1.0	1.0	1.3
Antenna LNA power output (VDC)	5	3.3	5	5	5	5	5
Antenna maximum current (mA)	200	200	200	200	200	200	100
Number of channels	136	132	132	120	120	120+24 (PPS)	120
Receiver clock error (ns)	10	10	10	20	20	20	20
Time to first fix (s)							
Cold start	45	45	45	50	50	50	50
Hot start	20	20	20	35	35	35	35

Table 3.1: Characteristics of the studied GNSS receivers

4 Antenna Selection

This chapter will discuss the antenna selection process. It will start by listing the antenna requirements. The antenna types and corresponding characteristics will be described. An initial selection will be made after which the link budget for these antennas will be calculated.

4.1 Antenna Requirements

The Antenna must meet several requirements coming from two different sources; the receiver and the system stakeholders, such as the satellite and the launch pod.

The requirements imposed by the receiver regarding the antenna are listed below:

AN-01 The GNSS Antenna shall be capable of receiving GPS L1 and L2 frequency bands.
AN-02 The GNSS data sampling rate shall be at least 1 Hz.
AN-03 The error in the determination of the antenna phase center shall be less than 10 mm.
AN-04 The antenna shall be an active antenna, so should have its own Low-Noise Amplifier (LNA).

From the other system stakeholders, the following subsystem requirements are defined:

AN-06 The GNSS antenna shall fit on the INS-1D satellite on an 45 mm by 45 mm square situated on top as illustrated in 4.1.
AN-07 The GNSS antenna may not exceed a height of 25 mm in order to fit in the INS-1D launch pod.
AN-08 The link margin for the GPS antenna shall be larger than 3dB [37].
AN-09 The GNSS antenna shall be able to survive 3 years in the space environment.
AN-10 The GNSS antenna may not be mounted by a magnet.

Soft requirements/trade-off criteria are:

AN-S01 It should be as light as possible.
AN-S02 It should be as compact as possible.
AN-S03 It should have a low LNA noise figure.
AN-S04 The link margin should be as high as possible.
AN-S05 The power consumption should be as low as possible.

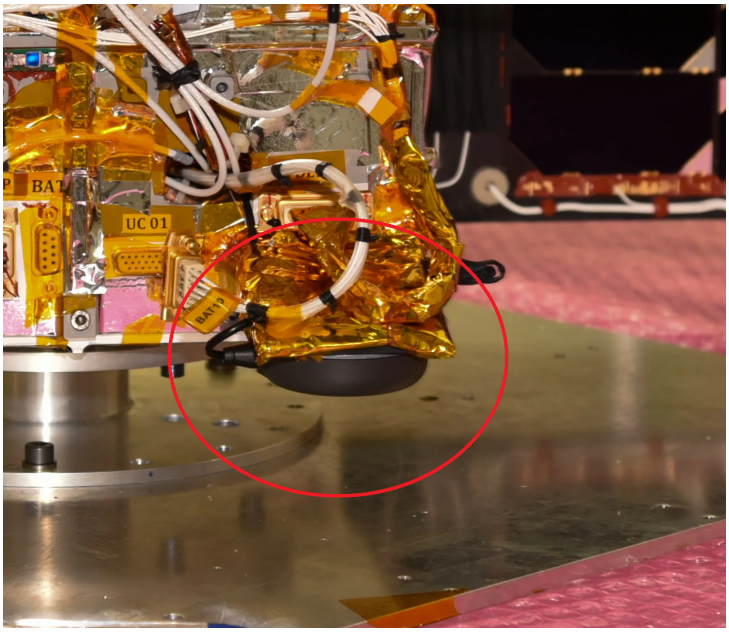

Figure 4.1: detailed view of the antenna mounting

4.2 Antenna types

An antenna can have various shapes and may or may not include electrical components. This section provides a main insight in the different types of antennas, their relevant shapes, and corresponding sizes. It will start by explaining why in this case an active antenna is required and what an active antenna is.

4.2.1 Active antennas

An active GNSS antenna contains one or multiple LNA and/or a pre-amplifier that boosts the signal strength of a weak received signal in order to re-enforce it for use by the GNSS receiver. This has several consequences: The most obvious one is that an LNA is an electrical instrument and thus requires power unlike a passive antenna. Therefore it needs to be incorporated in the power budget.

Another negative consequence of using an LNA is that it introduces additional noise. This will contribute to the total noise figure. Whether or not the received GNSS signal needs amplification is determined from the GNSS link budget as the potential antenna-receiver combination must yield a tolerant link margin ($>> 3\ dB$ [37]). This link budget is explained in section 4.3.

4.2.2 Antenna shape

A variety of antenna shapes exists, ranging from parabolic to bionic horn-like shapes as seen in figure 4.2. Some shapes are more applicable to CubeSats and Microstats than others. For example, parabolic antennas are often used on the ground for communication purposes. This is because parabolic antennas typically yield a high antenna gain (typically between 15 and 65 dBi [37]). Such a high antenna gain is not required for the GNSS receiver, as data rates are relatively low in this application. Furthermore, parabolic antennas are too large ($\sim m$) for this application.

A common antenna for receiving GNSS signals is the patch antenna. This type of antenna is for example used on the BlackJack receiver. It is easy to integrate with a CubeSat or Microsat due to its limited dimensions, which are in the order of centimetres. The fact that patch antennas are relatively inexpensive is an additional argument for selecting a patch antenna to accompany the receiver.

Figure 4.2: different antennas

4.3 GNSS link budget

The GNSS link budget is an approach that allows to account for signal power and noise power at relevant points in the GNSS transmitter-receiver system. For this application the carrier power to noise power spectral density ratio is calculated at the receiver. The link budget is determined with the gains for the zenith scenario with given system components. The noise figures of the components are selected at their maximum value, as supplied by the manufacturers.

4.3.1 Numerical model

The link budget that is presented in this section is based on the numerical approach developed by S. Rouquette [38].

Considering a single zenith mounted omnidirectional antenna, the theoretical radiation pattern is a half sphere meaning that the minimum elevation angle for tracking is 0°. The orbit simulation tool Systems Tool Kit (STK) was used to determine the maximum slant range at minimum elevation between receiver and transmitter simulated over a 3 year lifespan.

The carrier power to noise power spectral density ratio or Carrier-to-noise ratio (CNR) is the Signal-to-noise ratio (SNR) of a modulated signal. It can be formulated as seen in equation 4.1. It is dependent on the gain and power of the GNSS transmitter, the slant range between receiver and transmitter, carrier wavelength (L1 or L2), receiver antenna gain and receiver system noise temperature.

$$\left(\frac{C}{N_0}\right)_{dB/Hz} = 10\log P_s G_s - 20\log\frac{4\pi R}{\lambda} + 10\log\frac{G_r}{T_s} + 10\log L - 10\log k \tag{4.1}$$

With: $\frac{C}{N_0}$ the Signal to (reference) noise ratio , P_s and G_s power and gain of the satellite antenna,λ the Carrier wavelength, G_r the gain of the receiver antenna, T_s Receive system noise temperature,L

Additional losses and k Boltzmann constant.

The system temperature 4.2 depends on the reference temperature; which is the exposure temperature of the antenna, antenna noise temperature and the noise figure which is a measure of the degradation of the SNR. The noise figure is deduced from the data given by the antenna manufacturer.

$$T_s = T_a + T_0(NF - 1) \tag{4.2}$$

with: T_a Antenna noise temperature, $T_0$the Reference temperature and NF noise figure (receiver).
The antenna noise temperature is not physical temperature as in the actual temperature of the antenna in given circumstance but is parameter used to describe the actual noise contribution of the antenna in the system, in a given environment. This noise temperature is thus an other way to describe the noise induced by the antenna. It is dependent on the efficiency of the antenna, back to front ratio and the sky temperature. The back to front ratio is the ratio of power gain between the front and rear of a directional antenna. The sky temperature is in this case the cosmic background radiation.

$$T_a = \eta(T_{sky} + R_{bf}T_0) + (1 - \eta)T_0 \tag{4.3}$$

with: T_{sky} Clear sky temperature, R_{bf} Antenna back-to-front ratio and T_0 the Reference temperature

The additional losses 4.4 are dependent on the polarization losses and the reflection coefficient of receiver and transmitter antenna. The polarization match is the ratio between the left and right polarized radiation pattern. The reflection coefficient is the ratio of the reflected wave amplitude to the incident wave amplitude and can be obtained using the standing wave ratio specified by the antenna manufacturer.

$$L = p(1 - \Gamma_s^2)(1 - \Gamma_r^2) \tag{4.4}$$

with: Γ_s and Γ_r the antenna reflection coefficient for satellite and receiver.

The free space loss 4.5 is computed via the slant range and the carrier wave length.

$$L_p = 20 \log \frac{4\pi R}{\lambda} \tag{4.5}$$

with: L_p path losses,R distance traveled by the signal.

Finally, one is able to deduce the link margin 4.6 by subtracting the minimum required CNR for tracking and acquisition, which is a receiver parameter deduced by the manufacturer; in this case 35 dB and the calculated CNR.

$$M_{dB/Hz} = \left(\frac{C}{N_0}\right) - \left(\frac{C}{N_0}\right)_{min} \tag{4.6}$$

with:M_{db}/Hz the Link margin
finally the results of the theoretical calculation of the link margins for all frequency of the antennas under consideration can be found in 4.1.

Table 4.1: GNSS link budget

Symbol	Discription	I/O	Unit	Value			
				L1 GPS	L2 GPS	L1 GLONASS	L2 GLONASS
P_s	Satellite antenna power	I	dBW	16.5	16.5	16.5	16.5
G_s	Satellite antenna gain	I	dBi	13.8	13.8	13.8	13.8
R	Range	I	m	25350000	25350000	24250000	24250000
c	Speed of light	I	m/s	299792458	299792458	299792458	299792458
f_c	Carrier frequency	I	MHz	1575.42	1227.6	1602	1246
λ	Carrier wavelength	O	m	0.190293673	0.244210213	0.187136366	0.240603899
G_r	Receive antenna gain	I	dBi	4.1	0.5	2	-0.8
T_s	Receive system noise temperature	O	K	853.5	853.5	853.5	853.5
T_a	Antenna noise temperature	O	K	284.5	284.5	284.5	284.5
T_{sky}	Clear sky temperature	I	K	2.7	2.7	2.7	2.7
R_{bf}	Antenna back-to-front ratio	I	-	0.333333333	0.333333333	0.333333333	0.333333333
T_0	Reference temperature	I	K	284.5	284.5	284.5	284.5
NF	Receive noise figure	I	-	3	3	3	3
L	Additional losses	O	-	0.80256	0.8667648	0.8667648	0.8667648
p	Polarization match	I	-	1	1	1	1
Γ_s	Satellite antenna reflection coefficient	I	-	0.1	0.1	0.1	0.1
Γ_r	Receive antenna reflection coefficient	I	-	0.333333333	0.2	0.2	0.2
α	Atmospheric loss	I	-	0.912	0.912	0.912	0.912
k	Boltzmann constant	I	J/K	1.38E-23	1.38E-23	1.38E-23	1.38E-23
L_p	Path loss	O	dB	184.4752696	182.3084801	184.2352683	182.0523789
C/N_0	Carrier power to noise power spectral density ratio	O	dB/Hz	48.2586794	47.15970645	46.73291823	46.11580761
$(C/N_0)_{min}$	Minimal carrier power to noise power spectral density ratio	O	dB/Hz	45	45	45	45
M_{db}/Hz	Link margin	O	dB	3.2586794	2.159706451	1.732918226	1.115807614

4.3.2 Patch antenna selection and trade-off

The GNSS receiver antenna does not need a high gain, as it has to cope with relatively low data volumes. This means that a relatively inexpensive ($\sim$ 500-1000 Euro) commercially available patch antenna will suffice.

The criteria for the selection of possible antennas therefore focus mainly on size, weight and in a second order power. As discussed before in section 3 the receiver will use GPS and GLONASS in L1. This of course means that the antenna should be capable of receiving those signals ad the very least. With the mentioned criteria in mind several companies seem to provide suitable antennas. Some of them are dual frequency capable. Antennas from the following companies were considered: TRIMBLE, NovAtel, Tallysman and Antcom. A selection of the most suitable candidates and their characteristics are listed below in table 4.2.

Table 4.2: Reference antennas and corresponding characteristics

	1.3G1215A2-4.5NMM-4-SO1	GNSS-302L-A	TW2410	70229-XX
Manufacturer	Antcom (US)	NovAtel (CA)	Tallysman (CA)	TRIMBLE (US)
Frequency band	L1/L2	L1/L2	L1	L1
Antenna gain @90° (free space) (dBi):				
L1 GPS	0.4	3.3	4.25(with ground plane 100mm)	2
L1 GLONASS	0.4	2.7	4 (with ground plane 100mm)	2
L2 GPS	-2.2	3.1	NA	NA
L2 GLONASS	-2.2	1.5	NA	NA
LNA gain (dB):				
L1 GPS	24.0 (Option 43)	26	28	28
L1 GLONASS	24.0 (Option 43)	26	28	28
L2 GPS	24.0 (Option 43)	30	NA	NA
L2 GLONASS	24.0 (Option 43)	30	NA	NA
L1 GPS	100	100	unknown	100
3 dB Beamwidth (°):				
L1 GLONASS	100	100	unknown	100
L2 GPS	100	105	NA	NA
L2 GLONASS	100	100	NA	NA
LNA typical power	0.116	0.116	0.116	0.116
Noise figure LNA (dB)	1.8	3.0	1.5	2
Mass (g)	53	227	110	115
Length $\times$ width $\times$ height (mm)	$33.53 \times 33.53 \times 17.58$	$76.2 \times 119.3 \times 26.3$	$57 \times 57 \times 15$	$49.1 \times 46 \times 15.4$
Temperature (°C)	-55 to 85	-40 to 85	-40 to 85	-40 to 90

Looking at the size of different antennas we can see that only the Antcom antenna is meeting the size requirement AN-06. In fact the NovAtel antenna does not even meet the height requirement of 25 mm AN-07 all the other do. It should be noted when looking at the size of the NovAtel antenna that a mounting plate is included. The actual antenna has only a diameter of 66 mm which is still too large. However, we still include this antenna in the consideration since it is the only one of this group that has actually been used in space. It might thus be worthwhile looking to the possibility of enlarging the mounting area or slightly moving it. The TRIMBLE one does not meet the AN-10 requirement. It might be possible to remove the magnet. A version without magnetic mounting is also available but is considerably larger diameter of 63.3 mm and hight of 40 mm including a connection element. All antennas are made of ceramic materials and are easily expected to meet the 3 years survival requirement. All other requirements are met.

Several other remarks should be made regarding the date present in table 4.2. The free space gain of the Tallysman antenna was not provide by the manufacturer. A gain for a 100mmX100mm ground plane was given. When looking at the available data from other manufactures an extra gain of about $3dB$ can be expected. Therefore, in the link budget calculations 3 dB was subtracted from the values in the table 4.1. (see section 4.3) The beamwidth is not known either for the Tallysman. Because it is similar to the other antennas we can safely assume a beamwidth of 100 degrees.

The free space gain from the TRIMBLE are theoretical maximums, where the other ones presented the tested averages. The TRIMBLE values are thus expected to be lower then presented here in the table.

It should be noted that both LNA gain and LNA noise figure are frequency dependent. This can be observed by looking at the different gains in the different frequency bands for the dual frequency antennas. The gains represented in the table are the minimum gains, due to Doppler shifts of the incoming signals, the signals will experience unequal gains. Similarly,the LNA noise figure is conservative as the values in the table represent the maximum noise.

Taking the remarks from above into account we will now consider the link budget. The link budget for the different antennas was made by substituting the relevant parameters in the method of section 4.3. This is done to verify whether the potential antenna-receiver combination yields a sufficient link margin greater then 3 dB [37]. The obtained link margins for both the active and the passive antenna modes, are collected in table 4.3.

The antenna gain is used for the calculation of the passive link margins, whereas the LNA gain is used for the active link margins. It should be noted that the link margin calculated in table 4.3 for antennas are calculated without taking into account the effect of the ground plane as this would make virtually no difference for our configuration.

Table 4.3: Passive and active link margin for the 1.3G1215A2-4.5NMM-4-SO1, GNSS-302L-A, TW2410, 70229-XX antenna

	1.3G1215A2-4.5NMM-4-SO1	GNSS-302L-A	TW2410	70229-XX
Passive link margin (dB)				
L1 GPS	−2.4	3.59	−2.0	1.2
L2 GPS	−4.6	2.16	NA	NA
L1 GLONASS	−2.97	1.73	−1.1	1.2
L2 GLONASS	−4.92	−1.12	NA	NA
Active link margin (dB)				
L1 GPS	21.6	29.6	26.0	29.2
L2 GPS	19.4	28.2	NA	NA
L1 GLONASS	21.0	31.7	25.6	29
L2 GLONASS	19.0	28.9	NA	NA

Looking at the result in table 4.3, the NovAtel (second) appears to be the antenna with the best overall link margins. The NovAtel even seems to be able to perform passively for L1 GPS. For L1 GLONASS the tolerant link margin of greater then 3 dB [37] is not satisfied. However since the link margins for L1 GPS is still close to the 3 dB it is still advisable to switch the LNA on. The LNA only requires a limited amount of power and is essential for all the antennas to meet the required margins. It should be noted that the LNA typically scales up the signal as well as the noise linearly with the same factor.

On top of the up-scaled original noise some added noise is caused by the LNA. The amount of added signal noise is indicated by the LNA noise figure. To counteract the increased noise, the Novatel, Tallysman and TRIMBLE antenna have an active filter on their antennas LNA that also reduces some of the noise sources, mainly multipath errors by rejecting signals out of the selected frequency band. Although in the current satellite configuration the multipath induced noise is expected to be very small.

Finally it should be noted that the link margins in table 4.3 are calculated for tracking with maximum accuracy, requiring 35 dB signal to noise ratio as specified by the receiver manufacturer see appendix B. This means that for lower margins tracking the satellite is still possible but the accuracy will suffer.

Considering all the above if we do the trade-off, the winner would be the Antcom antenna, since it is the only one that meets all the original requirements and it has the second best performance. However, this is where things become complicated. During the design process of the satellite, the space provided for the antenna was slightly increased, allowing for a bigger antenna. The height requirement (AN-07) remains the same. This means that the NovAtel still remains out of consideration, but all the others become a possibility from space perspective.

The design team of the INS-1C selected the Tallysman, because they had previous experience with the manufacturer and the combination of this antenna with the receiver. Because this antenna was not immediately available for the testing, the largely similar TRIMBLE antenna was used for the static testing on Earth.

5 Testing different Configurations of the Receiver Antenna System

In this chapter we will first describe the general test approach and data handling protocol to produce comparable results. Then seven different tests that have been executed in static conditions are described and their key findings discussed. With those tests we will try to find an indication of the positioning accuracy that can be obtained with a Skytraq singe frequency receiver and the conditions that influence this. Finally, the receiver was tested in a GPS Signal simulator to mimic dynamic environment of a LEO orbit.

5.1 Test Approach

In the sections that will follow this introduction several tests will be performed in order to analyze the antenna-receiver combination that was used in mission INS-1C.

The first test is used to configure the test setup. Test 1 determines as accurately as possible the reference position that will be used for all later static tests. All subsequent static tests will use the measured distance deviation from this reference position to get a final impression of the positioning quality of the configuration and filtering strategy used with the considered test series.

From test 2 to 5, different configurations of the antenna-Skytraq S1216F8-GL receiver combination were tested in static conditions. We first analysed the performance of an antenna, TRIMBLE 70229-XX, very similar to the antenna used on the mission, but encased in order to protect it from weather conditions on Earth, in a configuration without ground plane. Secondly a large ground plane to simulate ideal ground plane conditions was used. Then a simulation of the ground plane as used in the satellite INS-1C design was executed. Finally a test was set up to analyze the potential of the receiver in combination with the best antenna available for use on Earth : LEIAT502 from LEICA.

Tests with the Skytraq receiver have been repeated at least 4 times. In this way we can investigate if the test is influenced by the constant evolution of the satellite constellation over time. It should be noted that the number of observations is highly dependent on the number of satellites that can be tracked at a given moment in time. As tests happen over prolonged periods of time (mostly 30 minutes), it is obvious that certain satellites may come into view and others get out of view. We will average out the results of the different test series in order to minimize the dependence of the outcome on a less favourable satellite configuration when comparing one test to another.

As the satellites close to the horizon under a very low angle proved to be influencing the results a lot, an additional analysis was made to investigate this effect by placing the antennas under an angle of 15 degrees to check antenna performance and the influence of the ground plane in test 6 and 7. This is of special importance in the near polar orbit of INS-1C. In this orbit, many satellites will be seen under a low elevation angle.

For the different Antenna-receiver combinations several test series were executed to investigate the stability of the positioning accuracy results while the satellite configurations were changing over time.

The static tests will give us an impression on how the mounting of the antenna will influence the quality of the observations. It will also indicate how stable the internal position calculations of the receiver are for the different test series, when compared with the results of the filtering and position calculations from reference programs such as GIPSY, as described in the next section on the data handling protocol 5.2. With the internal position calculations, the position calculation made by the receiver software, on it‘s internal processor, are meant.

The static tests can give us an idea about the quality of the results for different configurations of the detected satellites. This can be important information to derive a strategy to limit the amount of raw data to be transmitted from the satellite to Earth. However, the amount of relevant information that can be derived from static tests on Earth is limited given the very different conditions when compared with a fast moving satellite in a LEO orbit. That is why some additional test series are being analyzed while using a GPS simulator as described in test 8. This corresponds to the real conditions and has as a big advantage that some error generating influences can be excluded for analysis. However, there are also disadvantages. The simulator cannot take GLONASS satellites into account, while these could provide additional information with the Skytraq S1216F8-GL receiver. This is why the earlier static tests will offer some complementary insight.

In each of the test scenarios described in the following sections the particular observations and the conclusions we can draw from these will be discussed.

5.2 GNSS receiver Data Handling protocol

The data flows follow two different paths depending on their origin, as can be seen in the flowchart 5.1. Validation data form the LEICA SR520 receiver collected with both the validation high performance antenna LEIAT502 and the test antenna from the tested Skytraq receiver go through two conversion steps before following the same data handling protocol as the data from the Skytraq receiver.

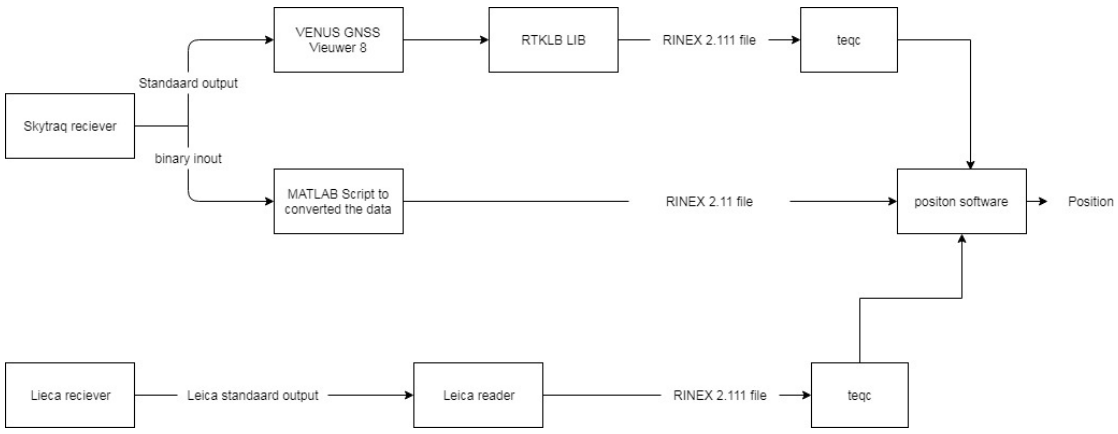

Figure 5.1: flowchart of the data processing

The Skytraq receiver data are collected in the test setup by the program GNSS Viewer with a custom release for this receiver: Customer Release-2.0.296 for Venus 8. For more information about this program, the background information section on GNSS Viewer can be consulted in chapter Data Analysis Software. It is important to acknowledge that this program won‘t be used on the actual mission. It is too CPU intensive and does unnecessary calculations on the raw data, such as an actual position calculation.

However, these unnecessary calculations during the mission are an advantage for this study since they allow for a direct visualization of the collected data. This makes it possible to do a first quality check during the actual collection of the data. GNSS viewer allows to get an idea about the number of

satellites tracked and the quality of their signal as well as the position of the satellites with respect to the antenna in real time.

During the actual mission the binary output will be directly collected and stored on the dedicated storage space in the satellite. The binary output is not transmitted real time, but can be downloaded on scheduled moments.

The next step in the test protocol is to import the collected data from the Skytraq receiver into RTKLIB, see flowchart 5.1. For more information on RTKLIB the background section on RTKLIB can be consulted in the chapter Data Analyses Software. The module of RTKLIB in this study will be RTKLIB convert which transforms the raw data from its binary form into three files of the RINEX format 2.11. The produced files are:

- a file with the observation data having extension .obs as prescribed by the Rinex standard
- a file with navigation data having extension .nav as prescribed by the Rinex standard
- a position file calculated by RTKLIB having extension .pos

We actually use only the first and second file. The third is a static position calculation made by RTKLIB. However, because we have access to GIPSY which is more accurate and has a wider range of possibilities, this file can be ignored.

From this point in the data flow, the data from the validation receiver and the Skytrack receiver follow the same path, see flowchart 5.1. The following step is to check the created RINEX files for mistakes and filter them to ensure data quality. For this purpose the *teqc* program is being used about which more can be found in section 2.4.

The data is inserted in the teqc standard quality checker *+qc*. Both .nav and .obs are checked by cross referencing each other and filtered according to certain thresholds. This step produces a report on the quality of the data. In appendix C an example of this report can be seen for data collected for the accurate position determination of the reference point used for testing.

Important in the use of teqc is the choice of the thresholds. For example in appendix C the minimum acceptable signal to noise rate is set as larger than 3 db. Limits are typically also set on the view angle (10 deg.) to reduce the influence of multipath and ionospheric delay. In this example case, a limit was set on the maximum rate of ionospheric delay of 400cm/min. Given these parameter in combination with some outlier removal done by teqc in the example of appendix C 2392 observations of the 30564 observations did not meet the quality requirements and were deleted. In this particular case plenty of observations are left to do a position determination. This will not be the case in all test setups. We will describe the choice of relevant threshold values for each individual experiment.

The next step is to insert the data in GIPSY which is described in the chapter section 2.5. A position calculation will then be made by GIPSY. This final position calculation will be used to analyze the performance of the receiver in the specified test circumstances. Additional conditions might be set in GIPSY to further investigate the performance: for example, the position calculation could be done without GLONASS or a specific GNSS satellite might be removed from the input data.

Finally we will compare the results of the different tests on the basis of distance calculations in Matlab with the help of the WGS84 coordinates system. When necessary the formulas described below were used to go from longitude, latitude and altitude to the elliptical WGS84 model. We need to 2 parameters to do this translation: the semi-major axis a and the eccentricity e[39].

$$a = 6378137m$$
$$e = 8.1819190842622 * 10^{-2}$$

To make the calculation easier we first calculated the The Radius of Curvature RC in the Prime Vertical, see equation 5.1.[40]

$$RC = a/\sqrt{1 - e^2 * sin(lat)^2} \tag{5.1}$$

With the latitude represented by lat in the equation 5.1.

The coordinates can then be calculated according to equations below:

$$\begin{aligned} x &= (RC + h) * cos(lat) * cos(lon) \\ y &= (RC + h) * cos(lat) * sin(lon) \\ z &= (1 - e^2) * RC + h) * sin(lat) \end{aligned}$$

where lon is the longitude and h the altitude in equation above.

5.3 Test 1: Determination of the exact position of the test point.

In order to do most of the subsequent tests a reference point has to be chosen. This point will be used to compare all further test results. It will be seen as absolutely correctly located. This point was localized as exactly as possible with the best possible equipment available at TU-Delft. The measurement was made with a LEICA SR520 receiver and the high performance antenna LEIAT502, also from LEICA.

In first instance, an attempt was made to locate the reference point on the roof of the Aerospace building at TU-Delft. The rooftop was chosen in order to avoid a ground-effect caused by radiation reflecting from earth and to avoid obstructions from other buildings on the campus. However, the rooftop of the building proved to be inaccessible in winter time and the wind-conditions were impacting both the building and the experimental setup. The technical concerns in combination with the fact that the roof was difficult to access since it required some one from building maintenance to be present at all time made us abandon this approach.

Consequently an alternative at ground-level was investigated. The reference location needed to have a minimum amount of obstructions at the horizon, so finally the location as indicated in Figure 5.2 was chosen.

Figure 5.2: Test location indicated by the red star

A tripod as shown on figure 5.3 used for map making and construction measurements, was then set up in the middle of this field. Next, the mounting plate of the antenna was leveled and the exact point above witch the antenna center would be placed was marked on the ground with a nail.

This nail indicated the reference point going forward for all subsequent tests. The position on the ground needed to be complemented with the exact altitude of the mounting plate to get also a fixed the vertical position above the earth surface. Since, it is already very challenging to get the tripod in a levelled position exactly above the reference point, an error of around 3 mm in the vertical position will need to be corrected for between the different test setups. The extent of this error was measured for each test setup individually with a measurement lint as indicated in picture 5.4.

Figure 5.3: Tripod [41]

Figure 5.4: Measurement lint

Figure 5.5: Measurement tool

It should also be noted that a second vertical correction should be applied to compensate for the vertical position difference that originates from a difference in antenna center height that results from a mounting difference between the different antennas. In order to know the exact vertical position of the reference test point the measured height in figure 5.3 should be added to the antenna center vertical height.

However, the software in the LEICA receiver compensates for the different types of antenna. When using a known antenna to this receiver it will always calculate the position of the mounting point. In other words the receiver will compensate for the antenna center offset. While in this test the LEICA SR520 is delivering the relevant results, it is important to notice for future tests that the Skytraq receiver is not making antenna based compensations to the mounting point.

The actual measurement was done by using the above described setup while measuring for 1 hour at a sampling rate of 1 second. This time frame was selected to avoid errors due to multipath, as well as to compensate for other kind of error sources as described in section 1.3 *Measurement Errors and their Mitigation*. The longer measurement time allows for the position to be calculated with multiple different satellites configurations and satellite positions, resulting in a reduced error in the position calculation.

The obtained data as extracted from of receiver can be found in appendix D. A total of 30564 data points was obtained. After filtering of the data as described in section 5.2 on GNSS receiver Data Handling, 2392 observation where deleted as they did not meet the quality requirements stated below:

- a minimum signal to noise ratio for L1 and L2 of 4 db
- a maximum ionospheric rate for L1 and L2 of 400cm/minute
- a multipath slip sigma threshold of 4.00 sigma
- a minimum view angle of 10 deg

For a detailed analyses produced by teqc see appendix D where you can find on what basis which observation was rejected, as well as the data overview. The observations where then loaded in GYPSY which produced the following exact positions in coordinates according to table 5.1 with respect to World Geodetic System 1984 (WGS84). WGS84 is the reference ellipsoid which is the basis of the reference coordinate system used by the Global Positioning System.

Table 5.1: Coordinates of the reference position

position	x	y	z
reference point (m)	3924421.3052	300264.4363	5002169.7403

The mean moving average root mean square (rms) of the position is less than 4.7 mm which gives an indication of the position precision. The position accuracy is harder to determine in this case since we don't not have an absolute reference point to compare the measured position to. The manufacturer gives an indication of systematic bias of about 5 mm on top of the random error [42]. We can assume this accuracy to be accurate enough for the type of tests we are describing below.

5.4 Test 2: Initial Testing of the Skytraq Receiver

Test 2 is executed to get first impressions of the accuracy of the Skytraq receiver in combination with the test antenna TRIMBLE 70229-XX. This test is executed in the same static conditions as those from the previous reference test.

Figure 5.6: the test setup for test 2

The Tripod setup is used. The antenna is directly connected to the receiver. The test setup can be seen in figure 5.6. This test was taking place on a different day than the one of test 1. However, the weather circumstances were quite similar.

Five test series were executed with each a duration of 30 minutes at a sample rate of 1 second. The total number of observations was about 30,000 on average. More details can be found in table 5.2 that lists the results for each test series.

A first remark is that we reduced the test duration because the initial test series lead to the conclusion that the position calculation results on the Skytraq converge already to stable values after approximately 20 minutes. Remarkable is that the Skytraq receiver tracks in 30 minutes approximately the same amount of observations as the Leica receiver does in 60 minutes. The Leica receiver is not tracking GLONASS satellites, it only considers GPS satellites. During test 1, it tracked 11 different GPS satellites.

The Skytraq receiver followed during the test 10 GPS satellites and 8 GLONASS satellites, 18 satellites in total. The data were processed according to the data-protocol described in section 5.2. When the data was put in teqc for quality control, approximately 6800 observations were rejected for not meeting the following quality requirements :

- a minimum signal to noise ratio for L1 and L2 of 4 db
- a maximum ionospheric rate for L1 and L2 of 400 cm/minute
- a multipath slip sigma threshold of 4.00 sigma
- a minimum view angle of 10 deg

Approximately two thirds of the observations are rejected because of the last quality requirement, a view angle above 10 degrees.

Even taking into account that there are more original observations in this test, due to the high amount of deleted, low quality, observations the final resulting number is lower than in test 1. A first explanation for the high rate of rejections is the smaller antenna with a more limited gain. A second explanation can be found in the different position of the GLONASS satellites which appear to be the most rejected ones.

Both these elements result in a lower signal to noise ratio increasing all errors. In thereotical circumstances even a third element could explain a higher amount of low quality observations generated by the Skytraq receiver compared to the Leica. The Leica receiver can only track 12 satellites, when this capacity is exceeded, the lowest quality observations will automatically be replaced. This leads to improvement in the data quality. The Skytraq receiver can track up to 28 satellites simultaneously and does not execute this replacement. However, given that in the test circumstances only 11 satellites were seen, this argument is here not valid.

The filtered results were introduced in GIPSY for the final position determination, they can be found in table 5.2.

Table 5.2: Deviations from the reference point with the different ionospheric models for the different test series

Test serie	1	2	3	4	5
observations	2948 2	29278	30626	30538	30024
deleted	6856	6642	6805	6908	6792
Deviations GIM (mm)	760	970	940	640	880
Deviations JPL (mm)	750	960	950	730	930

The average deviation of the position was 840 mm from the reference coordinates, with standard deviation of 123 mm. This is a significant difference which will be analysed below.

Looking at the results of the 5 test series, we observe a quite significant spread in accuracy. The worst value is close to 1 meter at 980 mm and the best result is 640 mm. These test where performed with the standard ionospheric model the GIM model. This is far from the centimetre accuracy that is envisaged with a dual frequency receiver for scientific purposes.

The Ionospheric delay is the largest single error source in position calculations for LEO satellites. Therefore the influence of the Ionospheric model that is used to correct for this error is very significant. In order to get an impression of the influence of the selected Ionospheric model, we will run the above data series through an alternative model than the GIM model from IGS. GIM is the most used model in literature and it is also the default choice in all of the experiments in this work.

The alternative model that was chosen is the JPL global TEC map. The calculation in GIPSY were repeated with the TEC map. This resulted in an average position error of 868 mm. Looking at the results we can see that none of the individual tests differ more than 100 mm between the different ionospheric models with the same test series and the standard deviation of the differences is 39 mm. In 2 of the 5 series we see a slight improvement of the result, while the 3 last ones show a slight accuracy deterioration. This indicates that the performance of both Ionospheric models is quite similar, the calculated positions are close together. The small differences can have many sources, for instance, the difference in update rate can be a partial explanation.

We also looked into the effect of leaving out the GlONASS observations on the position accuracy. We need to run a slightly different algorithm in GIPSY to do this. On top, a minimum number of observations and observed satellites is required. The time period had to be expanded to 1 hour in order to fulfill these conditions. In this case that implied that we had to combine data series 3 and 4 which where measured consecutively. In order to have a second data set for verification an additional test was done for 1 hour.

With GLONASS data included in the calculation the error was respectively 960 mm and 820 mm. It should be noted that the first data set was obtained on overcast day while the second was measured on a sunny day. This explains the significant larger error of the first one. The tropospheric conditions have an influence on the error, especially the wet component which is harder to model. The wet component is included in the tropospheric correction model we use here from the ECMWF. Note that the troposphere induced errors do not occur on the actual mission in LEO.

Removing GlONASS observations leads to a reduction in observations of about 40% in both cases. For the combined series 3 and 4 this means that 24348 of the 60752 observations were removed and for the new test 24886 of the 62420 observations. This resulted in a new position error of 970 mm and 820 mm. Immediately we can notice that there is not much difference although, there is a very slight deterioration in the first data, this far below the standard deviation of the original 30 minutes test series. This is judged as insignificant. Overall it can be concluded that extra GLONASS observations do not contribute. The choice of ionospheric model has more impact.

5.5 Test 3: Getting the most out of the Skytraq Reciever

In this test setup, we will try to create a configuration that enables to get the best possible results with the Skytraq Receiver, given the devices to which we have access. The Skytraq receiver will be connected to the Leica Antenna LEIAT502. The LEIAT502 is an active antenna that requires more power than the Skytraq receiver can deliver. As a consequence we needed to power the antenna with a separate battery during this test.

The observation period of this test was 30 minutes. It was executed 4 consecutive times. The test conditions where similar to the previous 2 tests. The data were analyzed according to the data handling protocol described in section 5.2. During the test 31500 observations were made and a total number of 18.5 satellites were tracked of which 12 were GPS satellites. It is obvious that the better antenna is also

giving a 5 % higher number of observations, due to the better quality of this type of antenna.

The data was put in teqc with the following quality requirements comparable to previous test:

- a minimum signal to noise ratio for L1 and L2 of 4 db
- a maximum ionospheric rate for L1 and L2 of 400 cm/minute
- a multipath slip sigma threshold of 4.00 sigma
- a minimum view angle of 10 deg

Only 7650 observations were removed by this quality filter of which 6200 are due to the 10 degree filter constraint. A lot of the extra data points are observations below the 10 degree threshold where lower quality signals can be expected. Overall, a higher usable number of observations is obtained then in the previous test. The relevant results are summarized in Table 5.3 under the header quality settings set 1, after being treated in the program GYPSY.

Table 5.3: Deviations from the reference point with different filter settings for the different test series in mm

test series	1	2	3	4
errors standard settings	480	470	610	510
errors with 8 db SNR	480	480	610	510
errors with 15 db SNR	470	470	580	510
errors with 35 db SNR	570	550	630	590
errors with 25 deg view angle	680	660	1020	650

We can observe that the accuracy is deviating 518 mm from the reference values obtained in test 1. As expected, giving the improved quality of the data by approximately one third, we find that a better antenna is reducing the position inaccuracy.

With this test setup we also did a sensitivity analysis on the influence of the quality parameters used for filtering in teqc. We wanted to understand the influence of the amount of observations versus the quality of those observations. This will also tell us something about the importance of the quality of the antenna

We ran teqc again with a variation in the quality requirements. The minimal signal to noise ratio for L1 is increased to 8 db. The resulting data, treated by GYPSY, are reported as Set 2 in the table 5.3. The much more stringent criteria results in a higher amount of rejected observations: 7800. This indicates that the lower signal to noise ratio signals are likely to be identical to those of the satellites that are located under the 10 degrees filter mask. Nevertheless there is an insignificant change in the obtained deviation from the reference point of test 1, in casu 520 mm. The 2 mm difference with the result of SET 1 is below the measurement resolution in the framework of our test program.

In a next experiment we increase the minimal signal to noise ratio for L1 further to 15 db. This is the same signal to noise ration that the Skytraq receiver is using in its own internal calculations. The amount of rejected observations is further increased to 8600. More than half of the observations are not strong enough to be maintained. The results of the GYPSY calculations are reported in table 5.3 under set 3.

Now we remark that the accuracy is further increased to 508 mm on average deviation from the reference position of test 1. This difference with respect to the 4 test series hides that for some tests, there is an improvement, but there is also an incidence of a worse result.

A further increase of the minimal signal to noise ratio for L1 to 35 db, results in the deletion of 17650 observations by teqc. In this situation the positioning accuracy is going down to 585 mm deviation,

which is still better than the result of test 2.

As most of the low quality segment can be associated with satellites that are low on the horizon, we also do some sensitivity analysis on the influence of the viewing angle quality criterion. In this experiment we increase the minimum view angle to 25 deg. The minimal signal to noise ratio for L1 is reset to 4 db in teqc. The GYPSY results are reported under set 4 in table 5.3. The amount of removed observations is rather high at 16800 and the position deviation is calculated at 753 mm. By analyzing the dataset closer we see that the inaccuracy is caused particularly along the North-South orientation. This result is not entirely unexpected as the reduction of the spread of the satellites taken into consideration for the position calculation is going to produce less accurate results and especially around the north and south poles, less satellites are being found. A factor that is further impacting the degradation of the accuracy is the more limited accuracy of the ionospheric models around the poles.

Out of this test it becomes clear that using a higher quality, bigger antenna will significantly the position accuracy, in this case by one third. In addition we can see that the best threshold for the signal to noise ratio is probably 15 db as used by the Skytraq own internal software.

5.6 Test 4: Standard ground plane

This test is a setup to determine the effect that a ground plane could bring on the gain of the test antenna. In this test a 10 cm by 10 cm ground plane is being used. This is the typical size used by manufacturers such as AntCom. The design of INS-1C does not feature a ground plane of similar size. This test wants to provide a reference for the potential loss that a limited ground plan may cause in the quality of the observations.

The antenna is placed in the center of this ground plane, as can be seen in figure 5.7 and 5.8. The typical gain of an antenna for such a ground plane is approximately 3 db. The additional gain varies depending on the frequency and view angle as is described in section 4 on the antenna.

Figure 5.7: test setup overview

Figure 5.8: detail of the ground plane

Test 4 is executed with the Skytraq receiver and the test antenna. The total test time is 30 minutes for each of 4 test series. This was done in accordance with the observations from previous tests that the conversion of the approximation of the location determination stops after 20 to 30 minutes on the Skytraq receiver.

During the test period of 30 minutes the average number of observations was about 27800. Detailed numbers are available in the table 5.4. The number of tracked satellites was on average 17 of which 9 GPS satellites. Test 2 had 30 000 observations. When looking in more detail at the observations of test 2, we noticed that on average there were 2000 observations with a view angle below 0 degrees in this test series. This indicates that the ground plane blocks the observations below 0 degrees view angle, but has no or very little impact on the number of observations above 0 degrees.

The data was processed using the data handling protocol as described in chapter 5.2. The quality requirements set in teqc were the same as for test 2 and 3.

This resulted on average in 3400 observations being rejected. The vast majority are rejected because they are below the 10 degrees view angle. While the total number of observations reduced with 7,5%, the number of deleted observations is more significantly reduced with 50%. In the end the total number of observations remained approximately the same. However, we noticed an increase in the signal to noise ratio for different view angles as shown in table 5.4.

Table 5.4: Deviations from the reference point with the different ionospheric models for the different test series

Test serie	1	2	3	4
observations	27450	27278	28326	28238
deleted	3282	3266	3625	3508
Deviations GIM (mm)	690	590	670	690
Deviations JPL (mm)	700	590	640	640

Comparing the final position calculated in this test with the reference position from test 1 results in a difference of 660 mm. More detailed results are given in table 5.4. This result is quite an improvement compared to the result of 840 mm deviation in test 2. This indicates that whenever possible a ground plane provides additional benefits in the position calculation, which are significant in the order of 15% to 20% improvements.

Also in the situation with the ground plane, the sensitivity of the results with respect to the choice of Ionospheric model was investigated. Previously mentioned results were based on the GIM model of IGS. The same calculations are performed in GIPSY with the alternative TEC model from JPL. The JPL average deviation was at 643 mm slightly lower, 17 mm, than the one from the GIM model. The standard deviation between the positioning results of the two models on identical data series was only 29 mm. Overall we can conclude that both models deliver very similar results and that the difference margins between both models are in the centimeter level range. Just as in test 2 the difference is not really significant, the deviations are quite random in positive and negative directions in the order of few percentages.

On the basis of these test data, we looked again briefly into the influence of GLONASS observations. We were again able to combine test series that where taken consecutively to one continuous 1 hour data set (serie 3 and 4). This resulted in an error with GLONASS of 690 mm and without GLONASS in a small improvement to 680 mm. Similarly to the equivalent experiment that was done on the basis of the datasets in test 3, we noticed also in test 5 that the dataset without the GLONASS data is approximately 40% smaller in size. This is quite considerable. Also this test enables to conclude that the influence of GLONASS seems to be insignificant.

5.7 Test 5: Actual ground plane simulation

In this test we are using the current design of the antenna ground plane on the satellite to test its effect on the position measurement. Figure 5.9 gives an illustration of the mounting plate of the antenna.

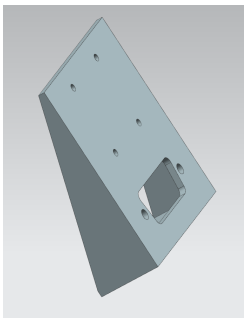

Figure 5.9: Mounting plate[43]

The antenna will be connected by the 4 screw-holes in figure 5.9. The plate to which the antenna will be connected measures 40x50 mm and it is further extended 25 mm to allow for cable connections. The hole for the cables will in the real installation be covered by a plate. The mounting plane is connected to the satellite bus which in itself also serves as ground plane extension with dimensions of 100 mm by 150 mm, see figure 5.10 and figure 5.11 .

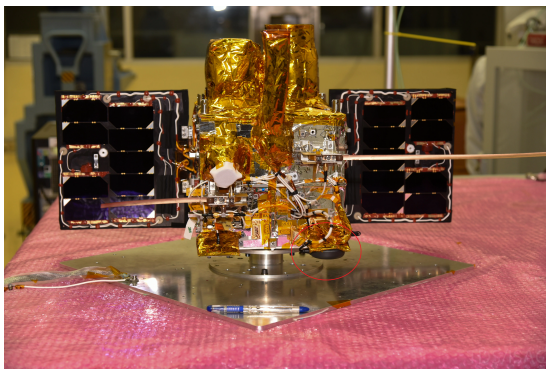

Figure 5.10: Configuration INS-1c [44]

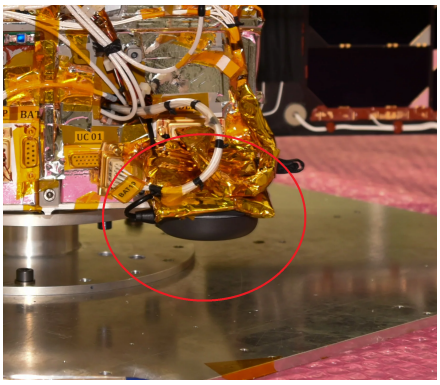

Figure 5.11: Configuration INS-1c detailed vieuw of the antenna [44]

This configuration was simulated as shown in figure 5.12. The antenna was mounted on a 40x75 metal plate connected to the ground plane as used in the previous test.

The test was executed in 4 series over a period of 30 minutes and on average 29550 observations were recorded. The data was processed according to section 5.2. In teqc the same filter values were used as in previous tests.

This resulted on average in 6900 observations being deleted. The majority, 3950, are being deleted because of the view angle constraint of 10 deg. This is a bit less than in the test 2 without ground plane. This indicates a small effect of the ground plane. The total number of useful observations is slightly less as in test 2, 22 650 versus 23 200 observations. The small difference of about 550 observations is due to a different number of satellites being tracked. It is important to remember that with the current sample rate one extra tracked satellite that is constantly in view during the test will result in 1800 extra observations.

Figure 5.12: Test setup

The data was processed in GYPSY resulting in table 5.5.

Table 5.5: Deviations from the reference point with Actual ground plane simulated

Test serie	1	2	3	4
observations	29382	29478	29326	30011
deleted	6482	6966	6872	7243
Deviations using GYPSY (mm)	840	840	820	780
Deviations receiver (mm)	9220	10060	8060	8210

The position deviation in comparison to the reference values of test 1 was on average 820 mm, a very small improvement on the 840 mm from test 3 without any ground plane. With this mounting configuration there is virtually no ground plane benefit. This can be explained by the fact that the antenna itself has already a 35 by 35 mm dimension and its packaging increases it to 45 by 45 mm. However it should be noted that the test antenna that we obtained is not fully identical as the antenna that would be used on the satellite. The test antenna has a weather protection cap and magnet mounting plate that increases its size compared to the one of the antenna configuration on the satellite. So the actual used antenna may still have a more beneficial effect from this mountain plate design.

Another conclusion that can be deduced from the growing number of rejected observations for other reasons that the minimal view angle constraint is related to the effect of the simulated satellite-bus configuration in the vicinity of the antenna. The large bus surface could induce a multipath error that explains the growing number of low quality observations between test 5 and 4, 2950 versus 100 observations rejected. Nevertheless, if the antenna could be mounted directly on the larger satellite bus plate it would have a more significant positive ground plane effect as demonstrated in test 4.

In this test we recorded also the position calculations done on the Skytrac receiver itself. These positions are the only ones that have been received from the INS-1C satellite before it went dead. Unfortunately, it went dead before it was able to send any raw data from the Skytraq receiver out of orbit to Earth. We make this check to have an idea about the quality level of the position data received from INS-1C.

If we take the average error calculation of all those positions with respect to the reference position of test 1, we notice an average deviation of 8900 mm, which means that Skytraq receiver position calculations are order of a magnitude worse. This is, as we expected, far beyond the error level that

would be acceptable for scientific application. This shows the value of post processing the raw data and demonstrates the value of the ionospheric and troposphere models. On top the deviations between consecutive position calculations can even vary more significantly as can be seen in figure 5.13.

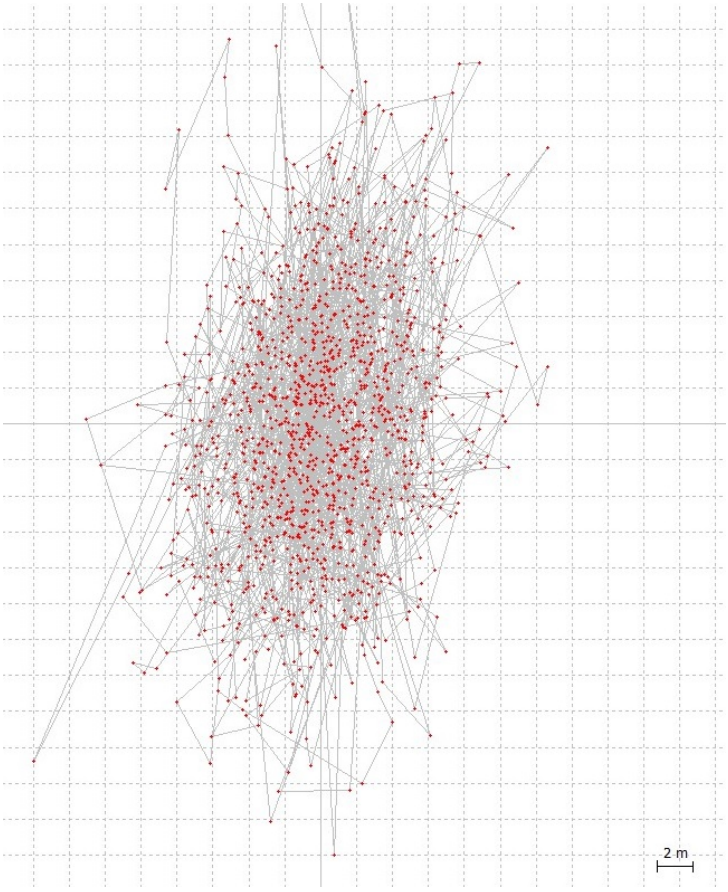

Figure 5.13: ground track of test 5

5.8 Test 6: Tilted satellite ground plane

In this setup the Skytraq receiver is being used with the test antenna and the real ground plane, extended with the satellite bus plane, placed under a 15 degrees angle with respect to the horizontal plane. The backside of the antenna is oriented towards the north. All other conditions are identical to those in test 5 with the simulation of the actual Antenna setup as being used on the satellite. The objective of this test is to investigate if signals low on the horizon can be observed and if this leads to any improvement. The setup is demonstrated in figure 5.12.

The test was executed 4 times over a period of 30 minutes. The standard data handling protocol of chapter 5.2 is being used. The quality parameters for teqc are put at the following reference values :

- a minimum signal to noise ratio for L1 and L2 of 4 db
- a maximum ionospheric rate for L1 and L2 of 400cm/minute
- a multipath slip sigma threshold of 4.00 sigma
- a minimum view angle of 10 deg

The initial amount of observations was 28750. This is 3% less observations than in test 5. This is due to the ground plane blocking out some observations to its backside. By orienting the backside of the antenna to the North we avoided getting less observations from the area above the North Pole that is less populated with satellites. The amount of deleted observations was 10400, which is significantly more than the 6900 deleted observations from Test 5 when the same quality parameters are used. 7650 observations were deleted because of the 10 deg minimum view angle criterion.

The satellites in front of the ground plane on a low angle with respect to the horizon are detected with a stronger signal influencing the reduction of low quality signals. In total we maintain 18350 observations which is 20% worse than the 22 850 observations of the previous test. The calculation in GYPSY results in table 5.6.

Table 5.6: Deviations from the reference point with a tilted satellite ground plane

Test serie	1	2	3	4
observations	29072	28378	29109	28492
deleted	7982	7366	7972	7263
Deviations cut off 10 deg (mm)	960	920	1230	810
Deviations cut off 25 deg (mm)	2020	1390	3590	1680
Deviations cut off 0 deg (mm)	890	780	920	860

The final distance result of the measured position, compared to the reference position of test 1, is 980 mm. This is despite the slightly higher number of observations a worsening of the positioning accuracy compared to test 5. This can be explained by the combination of the 15 degrees tilt with the 10 degrees cut-off angle that introduces a 25 degree reduction of the viewing angle to the backside of the ground plane. This implies that the field of view and consequently the spread of the observable satellites becomes more reduced which leads to a decrease in the accuracy of the position calculations in GYPSY.

It is especially indicative that the North-South error is increasing significantly from 880 mm in test 5 to 1320 mm in this test. This indicates once more the effect of a worsening configuration of satellites in the condition of this test. The same conclusion can be drawn from the position coordinates as calculated by RTKPLOT based on the raw data of the Skytraq receiver. These are represented in figure 5.14 for the different orientations. The deviations in the East-West orientation are less than half of those in the North-South orientation and very similar to those of the previous test. Note that the position results of RTKPLOT are an order of magnitude worse than those of GIPSY because no atmopheric correction models are used in RTKPLOT. Despite of the order of magnitude difference, the same trend as from GIPSY remains very apparent.

The negative effect of the inclination becomes even more outspoken if we increase the minimum view angle as a parameter in teqc to 25 degrees as indicated by the results of set 2 in table 5.6. The overall position deviation compared to the reference position is now 2170 mm. If to the contrary we reduce the minimum view angle to 0 degrees, we see a significant improvement of the position accuracy to 862 mm deviation from the reference point. When having a bad antenna orientation the filtering mask set in tecq is not giving any better results.

Overall we can conclude that placing the antenna under an angle is not beneficial for our tests on Earth. For a mission it is important to orient the antenna correctly perpendicular to Earth. If it is not possible to orient the antenna correctly, one has to be very careful with the selection of the minimal view angle filter mask. This filter can worsen the results if applied incorrectly.

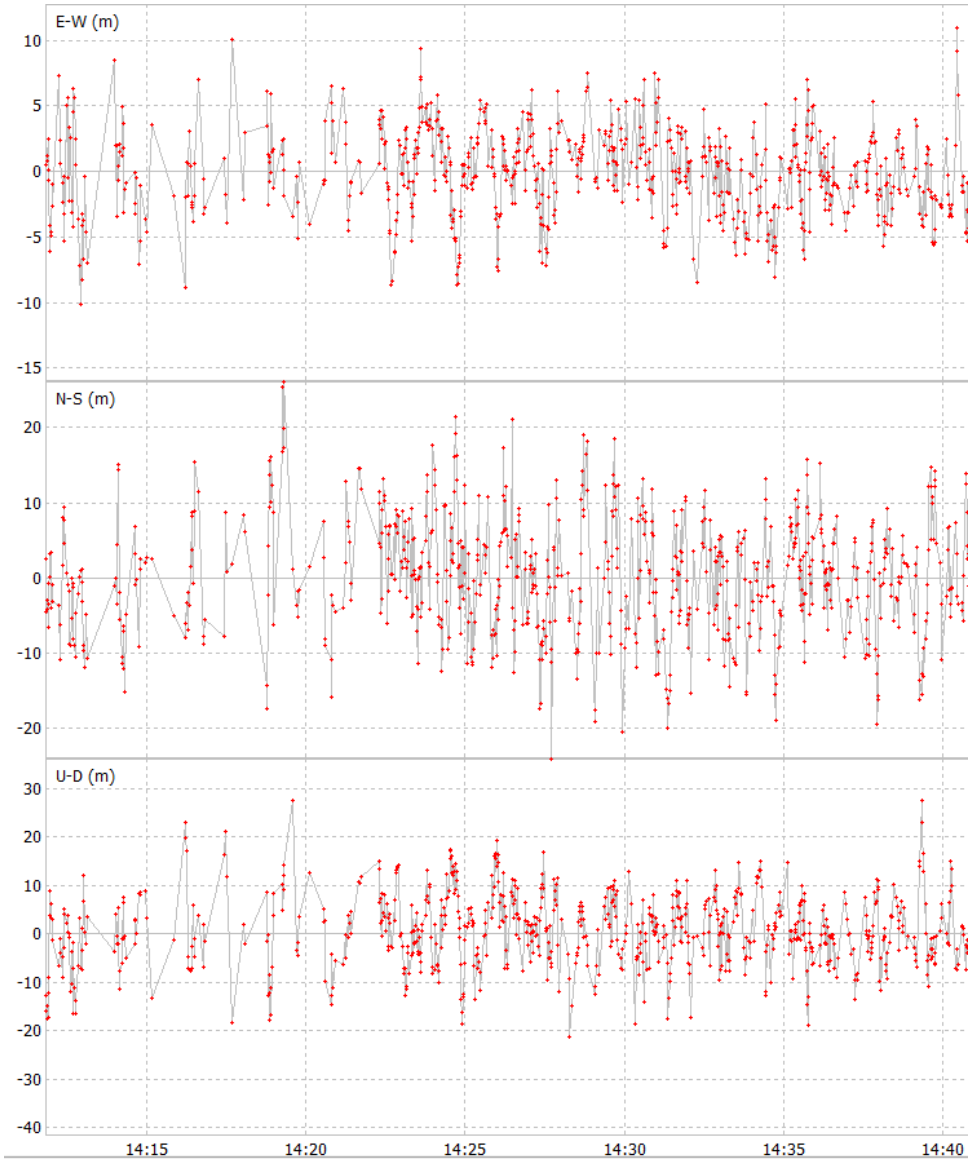

Figure 5.14: top: east-west, middle: north-south and bottom: vertical scattered plot

5.9 Test 7 : Tilted with reference antenna

Test setup 7 is a complementary experiment to test 6. With the previous experiment we investigated the ability of the Skytraq receiver and test antenna to track satellites under a low angle with respect to the horizontal plan touching the earth surface. In this setup we will use the best available antenna: Leica LEAT502 to verify if the satellites under these low angles are detectable anyhow.

In order to achieve approximately the same angular position with the Leica antenna as the one with the test antenna in test 6 we cannot use the satellite mounting simulation as this antenna has a different mounting system and it is too voluminous. The test conditions under the 15 degree angle are simulated by shortening one of the legs of the tripod. As a consequence, the tripod needs to be repositioned above the reference point provided by the nail in the ground. This approach is not as accurate to position the 15 degrees as the one of test 6. The estimated inaccuracy of the setup is estimated at 15 mm. The orientation of the angulation is exactly similar to the one of test 6 with the backside of the antenna oriented towards the north see figure /ref.

The test is performed during 4 periods of 30 minutes during which on average 30500 observations are recorded. The data handling protocol is followed as described in section 5.2. The quality parameters are set in teqc as in the previous tests.

This results in an average of 9100 deleted observations of which 8050 are deleted because of the 10 degree view angle, which is significantly more than the 7650 deleted observations from test 2 which happened without the tilted angle in similar conditions. The total number of observations is however close to the number in test 3 which had 31500 observations. This indicates that the Leica antenna is quite capable in tracking signals under a small angle. However, due to the increased viewing angle, adding 15 degrees tilt and 10 degrees cut-off towards the backside of the antenna, a bigger amount of satellite data on that backside of the hemisphere is deleted. This explains a reduced total number of useful observations with 10%.

Table 5.7: Deviations from the reference point with a tilted reference antenna

Test serie	1	2	3	4
observations	29964	31600	30437	30022
deleted	8782	9845	8972	8783
Deviations cut off 10 deg (mm)	540	520	590	580
Deviations cut off 0 deg (mm)	530	520	560	560

The calculation results of these input data in GYPSY are represented in table 5.7. The calculated difference position difference in this test with the reference position of test 1 is 558mm. This difference is with an inaccuracy of +/- 15 mm due to the difficulties of creating the exact setup as mentioned above. We notice that this result is in line with the expectations. It is very close to half of the deviation of the similar conditioned measurement in Test 6.

If we compare the results of test 7 and test 3 (520 mm). It is apparent that the reference antenna is less sensitive to a slight angulation as it is larger and more multi-directional. The reference antenna is also not influenced by the satellite ground plane that blocked a number of satellites in test 6.

In order to minimize the effect of the 15 degrees tilt angle on the + 10 degrees view angle cutoff, we execute the calculation once more with the minimum view angle set in teqc at 0 degrees. We notice a decrease of the deleted observations to 8250, which is giving us again a larger observation set to introduce into GYPSY. The results of this calculation are given in table 5.7. The deviation of the position calculation with respect to the reference position of test 1 is 543 mm. A small expected improvement over the previous result which also confirms the good omni-directional nature of the reference antenna.

5.10 Test 8: Receiver in the GNSS Simulator

All previous tests happened in a static environment and it is impossible on earth to fysically simulate the dynamic conditions of a LEO orbit. The dynamic behaviour of the satellite has an important impact on the receiver performance. It causes a Doppler shift of the incoming signals. This Doppler shift has multiple implications as mentioned in paragraph 1.4.1. In general this makes the tracking of GNSS satellites more difficult. It is therefore important that we characterize its effect on the receiver.

In order to execute this test, the following setup was made. The Skytraq receiver was connected to a GNSS signal simulator from the brand Spirent, model Global.[43] The simulater was configured to broadcast GPS signals only and directly connected to the receiver without an antenna. This implies that the antenna behaviour was not exactly simulated. The simulator provides us with accurate coordinates of the points along the orbit for which a flight trajectory is programmed. The main function of the simulator is to mimic the electronic signals that a receiver is supposed to receive when in space following this trajectory. This equipment is very expensive, so we could only get very limited access and data.

We were fortunate that PhD. student Sujay Narayana got unexpected access to the GNSS simulator at ISRO in India. This fortunate event was unknown to us, so we had no impact on the experimental setup and the executed experiments, but we have extracted maximum useful information in the context of this work from the obtained data.

In the current experiment, the simulated signal was broadcasted during 30 minutes and 10 seconds. The receiver only started up 31 seconds later. It took 11 seconds to calculate the first position fix. 6 more seconds were required to get a stabilization of the position fix. Overall it took 17 seconds to get a stable position fix, which is remarkably shorter then in most reference missions, e.g. CANX-2, see section 1.4.1. This makes using the receiver on board the satellite a lot more practical since re-establishing position fix is much faster. During the total test period 1758 positions were calculated at a sample rate of 1 second. A Matlab program was made to analyse the data coming from the simulation experiment. In this program we will compare the theoretical positions of the orbit that was provided as input to the GNSS simulator with the output data of the Skytraq receiver. All positions in the program will be expressed in the WGS 84 coordinate system. Unfortunately the data output from the Skytraq receiver during the simulation test did not allow to extract the raw data. This made it impossible to repeat the calculations in GIPSY.

If we use this Matlab program to study the positions calculated by the reciever we can start making the following observations, as displayed in figure 5.15:

Along the X-axis we notice at first instance an enormous error about half way through the testing period from second 837 to 839. The receiver looses track of several satellites and drops back to tracking only 2 satellites which is insufficient for a stable position fix. We see that the algorithm in the receiver tries to continue providing propagating position fixes. In figure 5.15 we see that the position is so far off the theoretic position, that the graph plotting the errors runs over 6 kilometers. This is caused by the very fast movement of the simulated satellite. From this we learn that we will have to be very careful with the positions fixes calculated by the receiver during its mission. The Doppler effect here causes a similar catastrophic effect as experienced during the CANX-2 missions described in section 1.4.1. Here we also find an example of a runaway error, but different from the experience during the CANX-2 mission, a cold restart can be avoided. After 3 seconds, the receiver manages to correct itself. It re-finds a sufficient amount of GNSS satellites to re-adjust its position fixes. Because these 3 seconds from 837 to

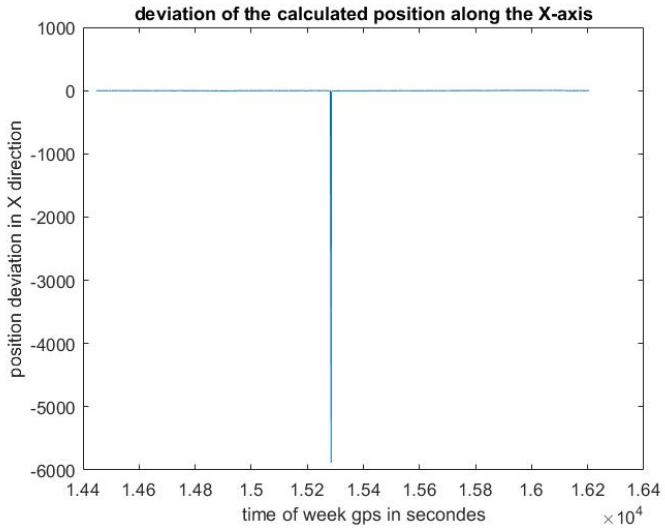

Figure 5.15: deviation of the calculated position along the x axis for the complete data set, excluding start up

839 present such large outliers in our data set we will remove the data obtained in this period in order to enable a better study of the remaining observations. Further discussions will be based on the remaining

data points only.

We observe an average error along the X-axis of 1.5 meter. The standard deviation of the error is quite large at 1.95 meter. When looking in more detail at the graph in figure 5.16, we observe that the graph shows a different behavior before and after the point where it looses a stable position fix. In the first part, we see that the X-position is systematically overestimated with an average error of 2.3 meter and a standard deviation of 0.85 meter. In the second part the X-position is underestimated with a deviation of 0.96 meter with a standard deviation of 2.4 meter. We notice here also a longer period of systematic drift that is being compensated at the end of the observation period. The difference in error pattern before and after the discontinuity in the measurement can be explained by the fact that during the discontinuity a new set of GPS satellites was tracked to base the Skytraq receiver calculations upon.

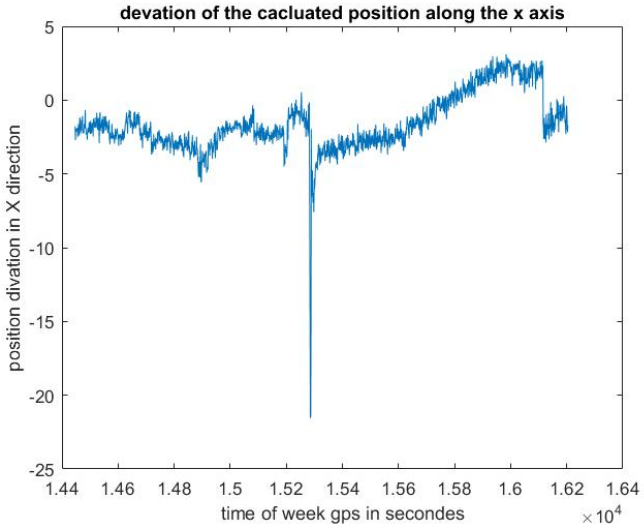

Figure 5.16: deviation of the calculated position along the x axis, without the data gap

The deviations along the Y-axis demonstrate a different pattern in figure 5.17. While the discontinuity is obviously also present, there is no obvious difference in the pattern of the deviations before and after the discontinuity. The mean error along the Y-axis is 10.2 meter and the standard deviation 9.9 meter. This is very substantial. The position fix is constantly drifting during the test period from an overestimation to an underestimation. However at the end of the period we see a slow stabilization. In the period after the discontinuity the deviation was 14.2 meter with a standard deviation of 3.7 meter. Here we have to be careful. If the drift of the error along the Y-axis would be continuous, this would require, after a while, a cold restart of the receiver during the mission. Unfortunately, the limited length of our data set does not allow to analyze this phenomena with more certainty.

The pattern of the deviations along the Z-Axis that can be observed in figure 5.18, looks a bit similar to the one along the X-axis. The average deviation along the Z-axis is 14.7 meter and the standard deviation is 3.7 meters. Similar to the deviation pattern along the X-axis, we observe that before the discontinuity, the deviation is relatively stable at an average value of 16.5 meter with a standard deviation of 1.9 meters. After the discontinuity we notice a drift towards a smaller error with an average deviation of 13 meter and a consequent larger standard deviation of 4.1 meter. The drift seems to stabilise at the end of our observation period.

Finally we calculated the distance of the measured positions compared to the reference positions. These distances are plotted in figure 5.19 and provide an impression of the total picture. The total average error is 19.1 meter with a standard deviation of 2 meter. Although the discontinuity results in a sudden jump of the distance of the deviation, the average deviation before and after are not that much different. Before the discontinuity the average deviation is 18 meter with a standard deviation of 2 meter

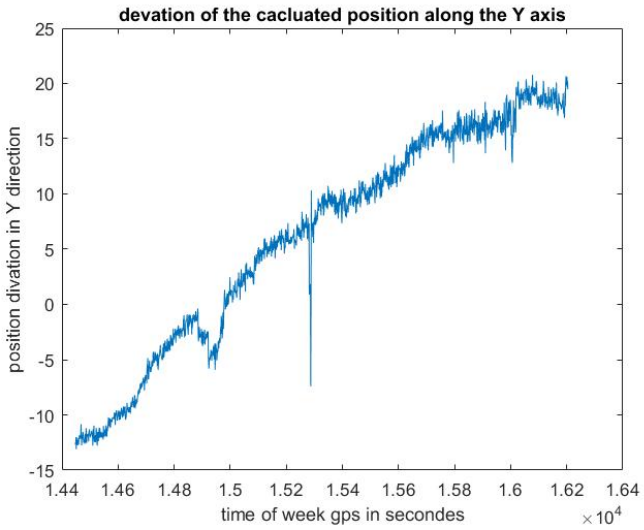

Figure 5.17: deviation of the calculated position along the y axis, without the data gap

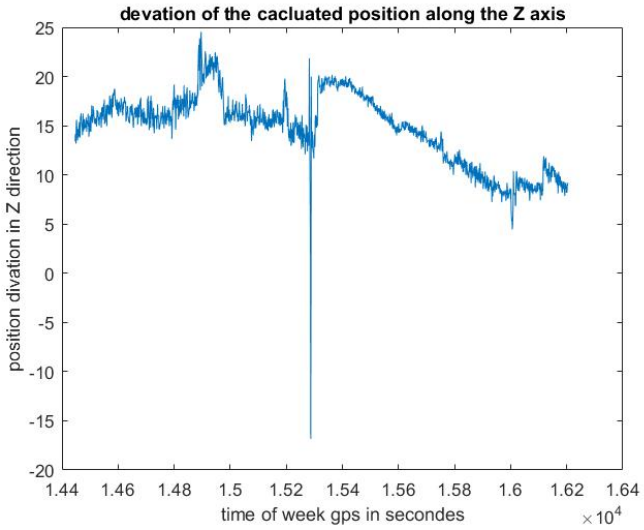

Figure 5.18: deviation of the calculated position along the z axis, without the data gap

and afterwards the average error is 20.1 meter with a standard deviation of 1.4 meter.

In summary we can conclude from this test that the TTFF of the Skytraq receiver is better then for previous used COTS receivers in space. This together with the fast re-establishing of a position fix after temporary tracking loss of a sufficient number of GNSS satellites is a strong characteristic of the Skytraq receiver which allows for continuous data sets. The receiver does seem capable of handling the increased frequency shifts caused by an increased Doppler effect well. This test was executed without GLONASS signals and did not appear to be suffering from it.

However, this data set with current single-frequency receiver is not providing sufficiently accurate data for meaningful scientific research results. The standard errors are still in the range of meters, even a dozen of meters. Scientific applications, such as gravitational research, require centimeter level accuracy.

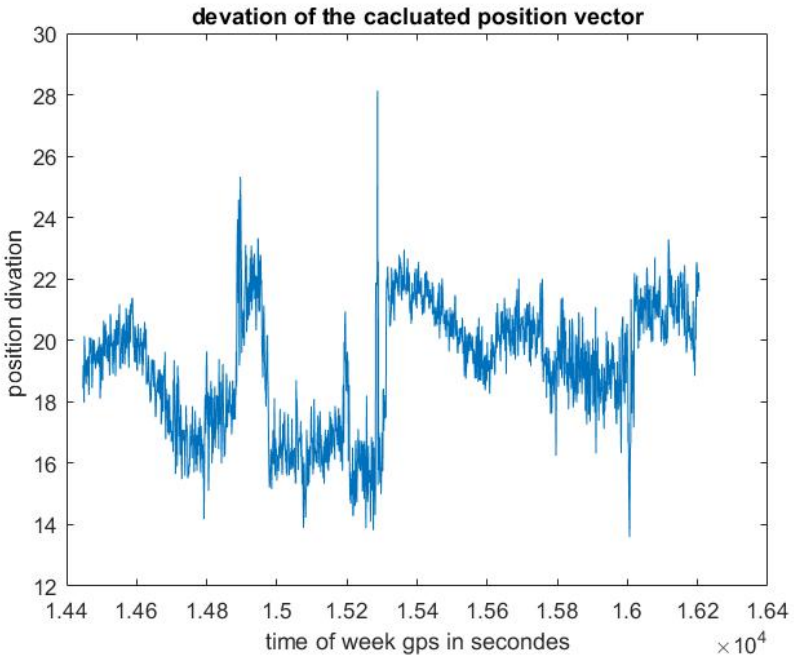

Figure 5.19: deviation of the calculated position, without the data gap

6 Conclusions

There are multiple ways in which accurate spaceborn GNSS satellite measurements can contribute to a variety of scientific topics. The number of applications has grown over the years since the launch of Landsat 4 in 1982 the first satellite with a GNSS receiver, to encompass wide variety of application in the fields of Earth sciences. The unique setup whereby the broadcast signals are man-made and controlled with a global coverage and then again received on other unique positions, allows the obtained measurements to be used in many different ways. This large flexibility and the global coverage has led to a wide range of scientific topics: ionospheric research, global hydrology, Earth gravitational field analysis, Thermosphere research, exosphere research and others. For example, the signal deformation and overall quality of the signal tell us something about the electromagnetic conditions in the atmosphere. That same signal can be used to determined the speed of the receiver which tells us something about the local atmospheric density.

There is room to make these measurements more cost effective by using COTS receivers. The current generation of space born GNSS receiver have given use insight in some of 21 century biggest challenges such as the insights provided by GRACE mission in the Earth's larger hydrological storage systems, understanding of this system is vital to understand rising sea level, droughts and so on. Study of the Earth's larger hydrological storage systems is just one area were GNSS receiver have contributed in our understanding of our own planet. Future price reduction in receiver cost would allow for a more continues in times and space availability of data and would future democratize the access to this data. This work aims to help contribute to the effort of reducing the price of spaceborn GNSS receiver by looking into COTS receivers. A collaboration with ISRO has given us the opportunity to effectively test and analyses such a COTS receivers.

In effort to contribute to insight of the viability COTS receivers for scientific applications this work addressed the following main research questions:

- Can relevant scientific information be derived from GPS measurements on a cubesat?
- What position accuracy of the current Antenna-Skytraq receiver as used on the INS-1C nano satellite can be obtained on Earth and what factors influence the position accuracy?
- What position accuracy can be achieved from an in space simulation of the Receiver System?
- What conclusions and design recommendations can be derived from the tests executed to answer the questions above?

The analysis performed in this work is an attempt to answer these questions. A collaboration with ISRO has given us the opportunity to effectively test and analyze such a single frequency receiver. As shown below, the obtained measurements indicated that position accuracy from a single frequency receiver is too limited for meaningful scientific applications. It is therefore rather a preparatory step to later move to a more accurate dual frequency COTS receiver in the frame of the INS series of Nanosatellites from ISRO.

The original hope to obtain a dual frequency GNSS receiver for testing, proved much more challenging than anticipated. Analysis of a multitude of commercial COTS dual frequency receivers in section 3 revealed that at the time of this research manufacturers were not able or willing to execute the necessary software adjustment to make their receiver space compatible.

In Skytraq we found a company willing to remove the COCOM restriction, the principal obstacle preventing us from using most GNSS receivers in space. During the initial testing period, Skytraq had no dual frequency receiver available, but was actively developing one which supposed to become released at the end of 2017. Unfortunately, due to delays in the development program, we were never able to test this receiver in the frame of this work. This limited all tests to the single frequency receiver that is currently used by ISRO and that also is used as basis for the new dual frequency receiver: the single frequency receive Skytraq S1216F8-GL.

This receiver was rigorously tested to find the influence of several design choices for the INS Nano-satellites. A first major conclusion is that the tests revealed that significant performance increases of the antenna can be made by including a ground plane. An increase in antenna performance leads to more observations of a better quality resulting in more accurate position determination. Test 4 revealed that the position accuracy improved more than 20% by using a standard ground plane in the test setup. Of course, a larger antenna yields even more gains in position accuracy, close to 40%. But it is not a practical approach, given the size restriction for flying an antenna on a Nano-satellite. Within the given size constraints for the antenna, there are multiple brands of COTS antennas such as: Antcom, NovAtel, Tallysman, Trimble, that can be selected as was analysed in chapter 4.

In the current INS-1C design, there is a minimal ground-plane that is just sufficient for placement of the antenna and that has no considerable positive influence, as could be seen in Test 5. It would be good to consider in the design of future INS satellite versions whether the antenna could not be mounted on the faceplate of the satellite bus. This faceplate has a good size for a ground-plane that would enhance the performance of the selected antenna with 20%. Obviously, this choice needs to imply that multipath errors caused by some of the other satellite components can be avoided as these would have a detrimental effect on the reliability of results.

Further research revealed that the choice of Ionospheric model in the data processing is not very significant as long as one of the high quality global models is used. This was proven by applying both the GIM model and JPL global TEC map model in test 2 and 4. The use of these Ionospheric and Tropospheric models on the raw data of the receiver is a requirement for obtaining any scientifically relevant position data. This was clearly observed in test 6 and 7 where the position data obtained from the Skytraq receiver itself showed deviations in the order of 10 meter, even exceeding 20 meter. This is consistent with the errors that can be expected by Ionospheric disturbance as described in more detail introductory section 1.2. Thanks to the use of the models in the post processing calculations on the raw data in GIPSY these errors were systematically reduced to sub meter level in all test conditions.

In all of the tests, the analysis of the cut-off angles revealed that it needs to be advised to keep the cut-off angle low, around 10 degrees,farther lowering introduce problems due multipath and limitations of the antennas design. Increasing the cut-off angle always reduces the position accuracy. The tests 6 and 7, where the antenna plane was tilted, demonstrated that low cut-off angles are important as a growing amount of observation data may be missed if the antenna is not directed to the zenith in a stable way. This situation might occur if the satellite itself is not perfectly stable, as was the case with the early INS satellite missions.

The use of GLONASS data is not instrumental to improve the accuracy of the position fix. In fact, in multiple data series of both test 2 and 4, with and without the ground plane, no significant contribution of the GLONASS data was found. This is important removing the GLONASS observations can to reduce the amount of raw data that need to be downloaded from the satellite for scientific calculations. In the datasets from the tests, this reduces the amount of data with approximately 40%, which is quite significant. We can notice that previous missions such as the CANX cubesat mission but also mission such as GRACE with a larger budget and satellites as described in the introductory section 1.4 also limited their data to GPS satellites.

An inclusion of GLONASS data could benefit the GNSS receiver‘s performance during the cold start procedure and avoid unwanted cold starts by lack of tracked satellites. The cold start, always coming up with an initial position fix within 20 seconds on the Skytraq receiver, never proved to be an issue

unlike it had been for some past missions with other receivers. For the mission described in section 1.4, recovering from a cold start took dozens of minutes, resulting in big gaps in the data set. The short terrestrial cold start time of about 20 seconds indicates that the Skytraq receiver is fast enough, even with the extreme velocities experienced on a LEO satellite, to obtain a position fix before the tracked satellites leave the field of view. This fast acquisition will allow the Skytraq receiver to deliver a much more continuous data set, even if a cold start would be required.

Test 8, with the simulator which simulated in orbit GNSS signal conditions, demonstrated that constant tracking with GPS satellites might result in sporadic loss of position fix. In theory the addition of GLONASS satellites should raise the chance of the receiver detecting a new satellite and thereby reducing the chance of loss of position fix. Although, this does not mean that the GLONASS raw data needs to be relayed to Earth.

Overall, we must conclude that a single frequency receiver has very limited applications for real scientific applications as all our tests demonstrated that they reach a sub meter accuracy at best during prolonged measurements. The realistic deployment conditions simulated in test 4 showed an accuracy of 0.6 to 0.7 meter, but this is a result obtained over a prolonged measurement time at the same position. In orbit the receiver is not stationary, but moving. Looking at the simulation test, an accuracy of 10 to 20 meter for in orbit conditions is more realistic. However, this meter level of accuracy in the single frequency receiver is a promising result to move within a dozen centimeter level of accuracy with a dual frequency receiver, which would allow much more scientific applications. The CASSIOPE mission discussed in section 1.4 has managed to validate that sub 10 cm level accuracy is possible with its 5 dual frequency NovAtel OEM4-G2L receiver setup.

7 Recommendations for future research

We are confident that the test framework with the different test setups used in this work can be used to do initial validations of the dual frequency receiver that is in development at Skytraq. This will immediately give an impression of the position accuracy gains that can be achieved and validate the specification claims made by the manufacturer.

In order to fully understand to what extent COTS receivers on LEO satellites can contribute to scientific research, relevant information can be obtained from missions that have used them. A mission like CASSIOPE has very recently delivered data from spaceborn COTS dual frequency receivers. A closer look at their results could be very beneficial. For now it has mainly been flown as a proof of concept. Its setup, with 5 receivers, generates a large data volume which means that most of the data is not transmitted back to earth. It would be very valuable to obtain data sets with continuous raw data, for a day or longer, from one or more of its receivers. This could reveal if the extraction of scientific relevant data is possible. Its in obit data in comparison with data from the same receivers tested on earth could also be used as a benchmark to validate test setups and simulations on earth.

CASSIOPE has already had the benefit that it can validate its accuracy by comparing the attitude obtained from GNSS measurements to its star-tracker obtained attitude. The accuracy of this comparison is limited by the accuracy of its star-tracker. Future INS missions could opt as a validation tool for Laser-retro reflectors instead of a star-tracker. This approach will obtain more accurate position precision estimates without the need to use multiple receivers to calculate the satellite attitude. This would save on data volume.

This work only looked at single and dual frequency receivers. As more and more GNSS satellites start to transmit in three frequencies, a look at triple frequency receivers might be worthwhile. For a first evaluation of the potential of these triple frequency receivers, similar tests as those done in this work could be used.

There are of course future improvements of our own the test framework possible, it would be good to extent the tests on the GNSS simulator. A first suggestion is to simply extent the test period significantly longer than 30 minutes. This would allow to estimate if the position loss is recurring regularly and under which conditions it is taking place. It also would allow to see if the drift in deviations that we observed in the limited data available becomes problematic. An additional benefit of a prolonged test period would be a better impression of the deviation-error patterns.

A second suggestion is to include GLONASS satellites in the simulated signals to investigate if this would resolve the loss of position fix that we have observed. In addition, one could also turn off the ionospheric interference simulation in the simulator. This would eliminate the ionospheric error from the signal and allow an optimistic estimation of the performance of the future dual or triple frequency receivers.

Finally we would like to repeat our suggestion for the serious consideration of the possibilities for the introduction of an antenna ground plane in future designs of the INS Nano-satellites.

8 Appendices

A Single and Dual-frequency Receivers for Space Applications

Table A.1: Dual-frequency GNSS receivers for space applications [45] [30]

Manufact.	Receiver	Chan	Ant	Power Mass	TID (krad)	Missions
Laben (I)	Lagrange	16×3 C/A,P1/2	1	30 W 5.2 kg	20	ENEIDE, Radarsat-2 GOCE
General Dynamics (US)	Monarch	6-24 C/A,P1/2	1-4	25 W 4 kg	100	
JPL (US) / BRE (US)	BlackJack / IGOR	16×3 C/A,P1/2	4	10 W 3.2/4.6 kg	20	CHAMP, GRACE, Jason-1/ COSMIC, TerraSAR-X
Alcatel (F)	TopStar 3000G2	6×2 C/A,L2C	1			Under development; PROBA-2
Austrian Aerospace (A)	Inn. GNSS Navigation Recv.	Up to 36 C/A,P1/2	2		>20	Under development; SWARM
BRE (US)	Pyxis Nautica	16-64 C/A,P1/2 L2C,L5	1-4	20 W 2.5 kg		Under development
NovAtel (CA)	OEM4-G2L	12×2 C/A,P2	1	1.5 W 85 g	6	CanX-2; CASSIOPE
Septentrio (B)	PolaRx2	16×3 C/A,P1/2	1 (3)	5 W 190 g	9	TET

Table A.2: Single-frequency GNSS receivers for space applications [45]

Manufact.	Receiver	Chan.	Ant.	Power Mass	TID (krad)	Missions
Alcatel (F)	TopStar 3000	12/16 C/A	1-4	1.5 W 1.5 kg	>30	Demeter, Kompsat-2
EADS Astrium (D)	MosaicGNSS	6-8 C/A	1	10 W 1 kg	>30	SARLupe, TerraSAR-X Aeolus
General Dynamics (US)	Viceroy	12 C/A	1-2	4.7 W 1.2 kg	15	MSTI-3, Seastar, MIR, Orbview, Kompsat-1
SSTL (UK)	SGR-05	12 C/A	1	0.8 W 20 g	>10	
	SGR-20	4×6 C/A	4	6.3 W 1 kg	>10	PROBA-1, UOSat-12, BILSAT-1
DLR (D)	Phoenix-S	12 C/A	1	0.9 W 20 g	15	Proba-2, X-Sat, FLP, ARGO, PRISMA
Accord (IND)	NAV2000HDCP	8 C/A	1	2.5 W 50 g		X-Sat

B | Skytraq Product Data Sheet

S1216F8-GL

High-Performance 167 Channel GLONASS + GPS Receiver

FEATURES

- 167 Acquisition/Tracking Channels
- Support QZSS, WAAS, MSAS, EGNOS, GAGAN
- 16 million time-frequency hypothesis testing per sec
- -148dBm cold start sensitivity
- -165dBm tracking sensitivity
- 29 second cold start TTFF
- 3.5 second TTFF with AGPS
- 1 second hot start
- 2.5m CEP accuracy
- Multipath detection and suppression
- Jamming detection and mitigation
- Self-aided ephemeris prediction
- Works with active and passive antenna
- Active antenna detection & short protection
- Operating temperature -40 ~ +85ºC
- Pb-free RoHS compliant

Applications

- Navigation / Tracking
- Timing reference

The S1216F8-GL is state-of-the-art global navigation satellite system receivers capable of tracking up to 28 GPS + GLONASS + QZSS + WAAS + EGNOS + MSAS + GAGAN satellite signals combined.

Dual-satellite navigation receiver module receives greater number of satellites than available for GPS-only receivers. The increased satellite number offers superior performance in challenging urban canyon and multipath environments.

The S1216F8-GL module contains SkyTraq Venus 8 positioning engine inside, featuring high sensitivity for indoor fix, low power consumption, and fast TTFF. The superior -148dBm cold start sensitivity allows it to acquire, track, and get position fix autonomously in difficult weak signal environment. The receiver's -165dBm tracking sensitivity allows continuous position coverage in nearly all application environments. The high performance signal parameter search engine is capable of testing 16 million time-frequency hypotheses per second, offering industry-leading signal acquisition and TTFF speed.

The S1216F8-GL module contains LNA for easy integration with passive antenna and a SAW filter for increased jamming immunity. It works with both passive and active antenna; the self-contained antenna detection and short circuit protection feature enables lowest integration cost for system integrators using active antenna.

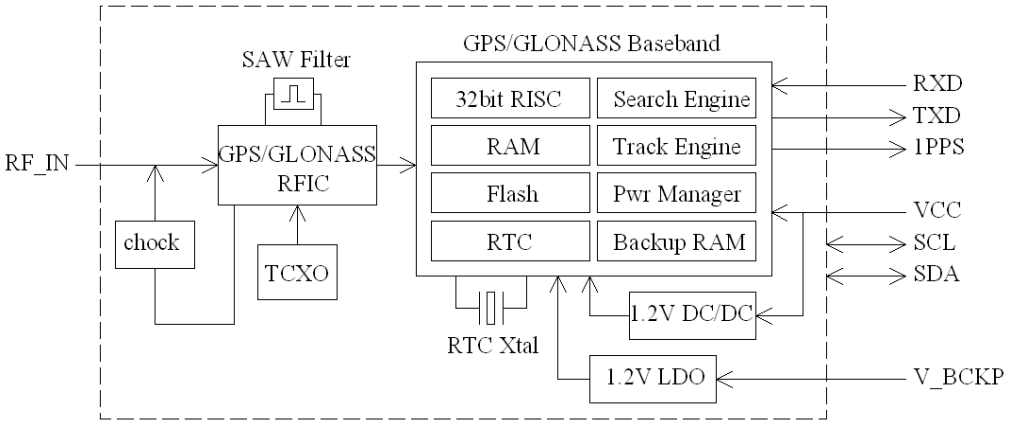

TECHNICAL SPECIFICATIONS

Receiver Type	L1 C/A, 167 channel
Modes	GLONASS GPS GLONASS + GPS
Accuracy	Position 2.5m CEP Velocity 0.1m/sec Time 10ns
Startup Time	1 second hot start < 29 second warm start 29 second cold start
Reacquisition	1s
Sensitivity	-148dBm cold start -165dBm navigation
Update Rate	1/2/4/5/8/10/20 Hz
Operational Limits	Altitude < 18,000m or Velocity < 515m/s
Serial Interface	3.3V LVTTL level
Protocol	NMEA-0183 V3.01 9600 baud, 8, N, 1
Datum	Default WGS-84 User definable
Input Voltage	3.3V DC +/-5%
Power Consumption	45mA@3.3V acquisition 40mA@3.3V tracking
Dimension	16.0mm L x 12.2mm W
Weight:	1.6g
Operating Temperature	-40^{o}C ~ +85^{o}C
Storage Temperature	-55 ~ +100^{o}C
Humidity	5% ~ 95%

ORDERING INFORMATION

Part Number	Description
S1216F8-GL	GLONASS/GPS Receiver

SkyTraq Technology, Inc.
4F, No.26, Minsiang Street, Hsinchu, Taiwan, 300
Phone: +886 3 5678650
Fax: +886 3 5678680
Email: info@skytraq.com.tw

C | Teqc Example Output

DLFT0470.18S

```
version: teqc  2018Jan11

 SV+--------------|------------------------------|-------------------------+ SV
  1|LLIccLI-LLL-LcLcL2LLILIcccM~III------------2~                           |  1
 13|L~~~~~~~~~~~~~~~~~~~~~~~~~~~~~~~~LIIII~IIcLLLIIc                       | 13
 12|L~~~~~~~~~~~~~~~~~~~~~~~~~~~~~~~~~~~~~~~~~~~~~~~~~~~~~~~~~~~~~~~~~~~~| 12
 15|L~~~~~~~~~~~~~~~~~~~~~~~~~~~~~~~~~~~~~~~~~~~~~~~~~~~~~~~~~~~~~~~~~~~~| 15
 17|L~~~~~~~~~~~~~~~~~~~~~~~~~~~~~~~~~~~~~~~~~~~~~~~~~~~~~~~~~~~~~~~~~~~~| 17
 19|L~~~~~~~~~~~~~~~~~~~~~~~~~~~~~~~~~~~~~~~~~~~~~~~~~~~~~~~~~~~~~~~~~~~~| 19
 24|L~~~~~~~~~~~~~~~~~~~~~~~~~~~~~~~~~~~~~~~~~~~~~~~~~~~~~~~~~~~~~~~~~~~~| 24
 10|L~~~~~~~~~~~~~~~~~~~~~~~~~~~~~~~~~~~~~~~IL2-LL----L----L-M~~~~~~~~~~~| 10
 25|          L     LcL    L LcI  LcLcI~LcII~~~~~~~~~~~~~~~~~~~~~~~~~~~~~| 25
 32|                             LcccccILLI~~~~~~~~~~~~~~~~~~~~~~~~~~~~~| 32
 14|                                                      LLccLIIccc     | 14
Obs|888888878887888889988888989998889999999999aa9898777787777889999999888|Obs
Clk|                                                                     |Clk
   +--------------|------------------------------|-------------------------+
14:46:04.000                                                    15:54:26.000
2018 Feb 16                                                      2018 Feb 16

**********************
QC of RINEX  file(s) : DLFT0470.obs
**********************

4-character ID          : DLFT
Receiver type           : LEICA SR520 (# = 20083) (fw = 5.10/1.039)
Antenna type            : LEIAT502        NONE

Time of start of window : 2018 Feb 16  14:46:04.000
Time of  end  of window : 2018 Feb 16  15:54:26.000
Time line window length : 68.37 minute(s), ticked every 30.0 minute(s)
Observation interval    : 1.0000 seconds
Total satellites w/ obs : 11
NAVSTAR GPS SVs w/o OBS :  2   3   4   5   6   7   8   9  11  16  18  20
                          21  22  23  26  27  28  29  30  31
Rx tracking capability  : unknown
Poss. # of obs epochs   :   4103
Epochs w/ observations  :   4103
Epochs repeated         :      0  (0.00%)
Complete observations   :  30564
 Deleted observations   :   2392
Obs w/ SV duplication   :      0  (within non-repeated epochs)
Moving average MP12     : 0.047560 m
Moving average MP21     : 0.062965 m
Points in MP moving avg : 50
Mean S1                 : 44.85 (sd=4.81 n=32956)
Mean S2                 : 47.09 (sd=3.21 n=30564)
No. of Rx clock offsets : 0
Total Rx clock drift    :  0.000000 ms
Rate of Rx clock drift  :  0.000 ms/hr
Avg time between resets : Inf minute(s)
Freq no. and timecode   : 2 13921 00c000
Report gap > than       : 10.00 minute(s)
       but < than       : 90.00 minute(s)
epochs w/ msec clk slip : 0
other msec mp events    : 0 (: 26)   {expect ~= 1:50}
IOD signifying a slip   : >400.0 cm/minute
IOD slips               :     34
IOD or MP slips         :     37
      first epoch    last epoch    hrs   dt  #expt  #have   %   mp1   mp2 o/slps
SUM 18  2 16 14:46 18  2 16 15:54 1.140   1     -   30564  -   0.05  0.06    826



Processing parameters are:
Receiver tracking capability       : unknown
Maximum ionospheric rate (L1)      : 400.00 cm/min
Report data gap greater than       : 10.00 min
```

```
              but less than       : 90.00 min
Expected rms of MP12 multipath    : 65.00 cm
Expected rms of MP21 multipath    : 65.00 cm
Multipath slip sigma threshold    : 4.00 sigma
% increase in MP rms for C/A | A/S : 100.00 %
Points in MP moving averages      : 50
Minimum signal to noise for L1    : 4
Minimum signal to noise for L2    : 4
Width of ASCII summary plot       : 72
Data indicators on summary plot   : yes
Do ionospheric observable         : yes
Do ionospheric derivative         : yes
Do multipath observables          : yes
Do 1-ms receiver clock slips      : yes
Tolerance for 1-ms clock slips    : 1.00e-002 ms
Do receiver LLI slips             : yes
Do plot file(s)                   : no

Observations start   : 2018 Feb 16 14:46:04.000
Observations  end    : 2018 Feb 16 15:54:26.000
Observation interval : 1.0000 second(s)
```

SV	#+hor	<ele>	#+mask	<ele>	#reprt	#compl	L1	L2	P1	P2	C1	C2
G10*	0	0.00	0	0.00	3247	3155	3247	3155	0	3155	3247	0
G12*	0	0.00	0	0.00	4103	4103	4103	4103	0	4103	4103	0
G13*	0	0.00	0	0.00	2583	2428	2583	2428	0	2428	2583	0
G15*	0	0.00	0	0.00	4103	4103	4103	4103	0	4103	4103	0
G17*	0	0.00	0	0.00	4103	4103	4103	4103	0	4103	4103	0
G19*	0	0.00	0	0.00	4103	4103	4103	4103	0	4103	4103	0
G24*	0	0.00	0	0.00	4103	4103	4103	4103	0	4103	4103	0
G01*	0	0.00	0	0.00	1294	390	1294	390	0	390	1294	0
G25*	0	0.00	0	0.00	2528	2036	2528	2036	0	2036	2528	0
G32*	0	0.00	0	0.00	2286	1888	2286	1888	0	1888	2286	0
G14*	0	0.00	0	0.00	503	152	503	152	0	152	503	0

```
   * = SV with no NAV info (or not being used)
Obs reported w/ code | phase  :  32956
Obs deleted (any reason)      :   2392
Obs complete                  :  30564

                                | G  |
% Obs            w/ no L1     :  0.0
% Obs            w/ no L2     :  7.3

% Obs            w/ no P2     :  7.3
% Obs            w/ no C1     :  0.0

% Obs            w/ low L1 S/N: 100.0
% Obs            w/ low L2 S/N:  92.7

No. of Rx clock offsets : 0
Total Rx clock drift    :  0.000000 ms
Rate of Rx clock drift  :  0.000000 ms/hr

MP12 RMS summary (per SV):
```

D | Raw Data Sample

```
$GNGGA,161753.999184,5159.3759,N,00422.6637,E,1,13,0.9,6.8,M,44.8,M,,0000*7C
$GNGLL,5159.3759,N,00422.6637,E,161753.999184,A,A*74
$GNGSA,A,3,26,29,05,16,20,31,25,21,,,,,1.7,0.9,1.4*2F
$GNGSA,A,3,82,73,80,83,81,,,,,,,,1.7,0.9,1.4*22
$GPGSV,3,1,11,04,83,186,49,26,73,277,48,21,63,163,46,16,44,300,45*7D
$GPGSV,3,2,11,29,41,072,47,31,30,206,43,20,19,130,38,05,16,040,43*70
$GPGSV,3,3,11,27,14,261,30,25,13,129,39,23,02,297,*45
$GLGSV,3,1,09,82,71,029,45,80,55,189,41,73,53,309,45,83,49,243,46*6D
$GLGSV,3,2,09,81,21,050,44,66,15,062,,65,12,005,29,74,06,332,*6B
$GLGSV,3,3,09,79,00,161,*54
$GNRMC,161753.999184,A,5159.3759,N,00422.6637,E,0.000,090.8,270418,,,A*4A
$GNVTG,090.8,T,,M,0.000,N,0.000,K,A*12
$GNZDA,161753.999184,27,04,2018,00,00*71
```

Figure D.1: fragment of raw data that has not been converted

```
     2.11           OBSERVATION DATA    M (MIXED)           RINEX VERSION / TYPE
RTKCONV 2.4.2                           20180429 081105 UTC PGM / RUN BY / DATE
log: C:\Users\dell\Documents\GNS\GNSS_Viewer\grounded.out   COMMENT
format: SkyTraq                                             COMMENT
                                                            MARKER NAME
                                                            MARKER NUMBER
                                                            OBSERVER / AGENCY
                                                            REC # / TYPE / VERS
                                                            ANT # / TYPE
  3924427.3433   300435.8973  5002127.6913                  APPROX POSITION XYZ
        0.0000        0.0000        0.0000                  ANTENNA: DELTA H/E/N
     1     1                                                WAVELENGTH FACT L1/2
     4    C1    L1    D1    S1                              # / TYPES OF OBSERV
  2018     4    27    16    18   12.2710000     GPS         TIME OF FIRST OBS
  2018     4    27    17    26    6.9940000     GPS         TIME OF LAST OBS
                                                            END OF HEADER
 18  4 27 16 18 12.2710000  0 16G 4G26G29G 5G16G20G31G25G21G27R18R 9
                                R16R 1R19R17
 101591186.236     -422827.330        1873.000          49.000
 101944257.329     -615405.336        3062.000          48.000
 103281868.172       21168.916        -228.000          47.000
 105530434.860     -274236.238        1263.000          43.000
 103048582.894     -714587.794        4822.000          45.000
 105164716.320    -1163214.480        5445.000          38.000
 104517075.204      101110.066        -842.000          43.000
 106148795.663      243958.437       -1288.000          39.000
 102754045.136     -737421.106        3395.000          46.000
 105478889.360     -525072.9451       5702.000          30.000
 100840373.418     -261999.196        1082.000          45.000
 101636412.344     -946199.602        4452.000          45.000
 101505668.346       -4263.165        -210.000          41.000
 104944476.934      -77796.5131        981.000          29.000
 101861490.232    -1059250.082        4899.000          46.000
 104023702.334      259399.792       -1372.000          44.000
 18  4 27 16 18 13.2710000  0 16G 4G26G29G 5G16G20G31G25G21G27R18R 9
                                R16R 1R19R17
```

Figure D.2: the same fragment of raw data that has been converted with the help of RTKB to RINEX similar looking NAV and GNAV file have also been extracted

Bibliography

[1] Xoneca, "Geometric Dilution Of Precision.svg," https://commons.wikimedia.org/wiki/File:Geometric_Dilution_Of_Precision.svg, 2013.

[2] System, E. O., "LANDSAT 4 (TM) Archive: 1982 - 1993," 2018.

[3] J., K. H., "CanX-2 (Canadian Advanced Nanosatellite eXperiment-2)," https://earth.esa.int/web/eoportal/satellite-missions/c-missions/canx-2, 2012.

[4] Ubox, "GPS Antennas locate, communicate, accele rateRF Design Considerations for u-blox GPS Receivers Application Note," 2009.

[5] Department of Space Indian Space Research Organisation, "INS-1As," https://www.isro.gov.in/Spacecraft/ins-1a, 2017.

[6] Department of Space Indian Space Research Organisation, "ISRO Nano Satellites," https://www.isro.gov.in/pslv-c37-cartosat-2-series-satellite/isro-nano-satellites, 2018.

[7] Skytraq, "GNSS Viewer for Venus 8 User Guide," /urlhttp://navspark.mybigcommerce.com/content/GNSSViewerUse

[8] Seco, "GNSS Instrument Tripods," /urlhttps://www.surveying.com/en/products/instrument-tripods.html?market=282p=2.

[9] Narayana S., "personal conversation," Phd. student EWI Tudelft contact person for INS programe and ISRO.

[10] Department of Space Indian Space Research Organisation, "ISRO," https://www.isro.gov.in/, 2018.

[11] Coias J. M. M., *Attitude Determination Using Multiple L1 GPS Receivers*, Master's thesis, Universidade Tecnica de Lisboa, 2012.

[12] Fattahyani, Ariadad and Grondman, Fabian and Houf, Daan and Kiyani, Bushra and Lubbers, Stephanie and Orsel, Erik and Roorda, Evelyne and Vancraen, Sander, *Gravity Explorer Satellite (GES), Providing data on temporal changes in Earth's gravity field for scientific use at low cost*, Master's thesis, TUDelft, 2014.

[13] Van Sickle, J., "GEOG 862 - GPS and GNSS for Geospatial Professionals,Lesson 2: Biases and Solutions," https://www.e-education.psu.edu/geog862/node/1596, 2018, part of Penn state's Master of Geographic Information Systems.

[14] Montenbruck O., Markgraf M., Garcia-Fernandez M., Helm A., "GPS FOR MICROSATELLITES STATUS AND PERSPECTIVES," *6th IAA Symposium on Small Satellites for Earth Observation*, April 2007.

[15] Montenbruck, O., Garcia-Fernandez, M., and Williams, J., "Performance comparison of semicodeless GPS receivers for LEO satellites," *GPS Solutions*, Vol. 10, No. 4, Nov 2006, pp. 249–261.

[16] Huba, J., Schunk, R., and Khazanov, G., *Modeling the Ionosphere-Thermosphere*, Geophysical Monograph Series, Wiley, 2014.

[17] OCEANIC, N. and ADMINISTRATION, A., "CURRENT SPACE WEATHER CONDITIONS," https://www.swpc.noaa.gov/phenomena/ionosphere, 2014.

[18] Wouters, B., Bonin, J. A., Chambers, D. P., Riva, R. E. M., Sasgen, I., and Wahr, J., "GRACE, time-varying gravity, Earth system dynamics and climate change," *Reports on Progress in Physics*, Vol. 77, No. 11, oct 2014, pp. 116801.

[19] Tapley, B. D., Bettadpur, S., Ries, J. C., Thompson, P. F., and Watkins, M. M., "GRACE Measurements of Mass Variability in the Earth System," *Science*, Vol. 305, No. 5683, 2004, pp. 503–505.

[20] Moore, P., Zhang, Q., and Alothman, A., "Recent results on modelling the spatial and temporal structure of the Earth's gravity field," *Philosophical Transactions of the Royal Society A: Mathematical, Physical and Engineering Sciences*, Vol. 364, No. 1841, 2006, pp. 1009–1026.

[21] Kramer H. J. , "GRACE (Gravity Recovery And Climate Experiment)," https://earth.esa.int/web/eoportal/satellite-missions/g/grace#foot3%29.

[22] Sunehra D., "Estimation of Prominant Global Positioning system measurement errors for GAGAN applications," *European Scientific Journal*, Vol. 9, No. 15, May 2013, pp. 68 to 81.

[23] Orus, p. R., "Ionospheric error contribution to GNSS single-frequency navigation at the 2014 solar maximum," *Journal of Geodesy*, Vol. 91, No. 4, 2017, pp. 397–407.

[24] Radicella, S., Nava, B., and Coïsson, P., "Ionospheric models for GNSS single frequency range delay corrections," *Física de la Tierra*, Vol. 20, 01 2008.

[25] JPL, "Global Ionospheric (TEC) Maps," /urlhttps://www.gdgps.net/products/tec-maps.html.

[26] Azab B., et. al., "Precise Point Positioning Using Combined GPS/GLONASS Measurements," *Geodetic Applications in Various Situations*, 2011.

[27] GMV, "Space Applications," http://www.navipedia.net/index.php/Space_Applications#cite_note-2, 2011.

[28] Global Aerospace and Defense Research Team at Frost and Sullivan, "Small-satellite Launch Services Market, Quarterly Update Q1 2018, Forecast to 2030," 2018.

[29] Leyssens J.,Markgraf M., "Evaluation of a Commercial-Off-The-Shelf dual-frequency GPS receiver for use on LEO satellites," Tech. rep., Septentrio NV and DLR, september 2005.

[30] Kahr E., Montenbruck O. , O'Keefe K. , Skone S., Urbanek J., Bradbury L., Fenton P. , "GPS TRACKING ON A NANOSATELLITE, THE CANX-2 FLIGHT EXPERIENCE," *8th International ESA conference on Guidance, Navigaion and Control Systems*, ESA, jun 2011, p. 1 to 8.

[31] Johnston-Lemke B., Z. R. E., "Attitude Maneuvering Under Dynamic Path and Time Constraints for Formation Flying Nanosatellites," *Proceedings of the 24th Annual AIAA/USU Conference on Small Satellites*, Aug 2010, p. 9 to 19.

[32] Markgraf M., Montenbruck O., "Total Ionizing Dose Testing of the NovAtel OEM4-G2L GPS Receiver," Tech. rep., DLR, December 2004.

[33] Lefebure,L., "How many GPS channels make sense?" /urlhttps://electronics.stackexchange.com/questions/11884/how-many-gps-channels-make-sense, http://lefebure.com/, novatel reseller.

[34] Montenbruck, O., Hauschild, Andréand Langley, R. B., and Siemes, C., "CASSIOPE orbit and attitude determination using commercial off-the-shelf GPS receivers," *GPS Solutions*, Vol. 23, No. 4, Aug 2019, pp. 114.

[35] N2YO.com, "INS-1C," https://www.n2yo.com/satellite/?s=43116, 2018-..

[36] Brčić, D., "RINEX-based GNSS positioning performance data analysis using the open source tool," *United Nations/Croatia Workshop on the Applications of Global Navigation Satellite Systems*, April 2013.

[37] Takasu, T., "RTKLIB: An Open Source Program Package for GNSS Positioning," http://www.rtklib.com/.

[38] UNAVCO, NASA, "TEQC," https://www.unavco.org/software/data-processing/teqc/teqc.html.

[39] Van der Marel H., De Bakker P.F., "GNSS Solutions: Single- versus Dual- Frequency Precise Point Positioning," *Inside GNSS*, 2012.

[40] Novatel Customer Service, "Personal communication," December 2017.

[41] Wertz J.R., Larson W.J., *Space Mission Analysis and Design*, chap. Communications Architecture, Space Technology Library, Microcosm Press, Springer, third edition ed., 2010, pp. 533–575.

[42] Rouquette R. E., "GPS L1 Link Budget," 2008.

[43] National Imagery and Mapping Agency, "Department of Defense World Geodetic System 1984: its definition and relationships with local geodetic systems," Tech. Rep. TR8350.2, National Imagery and Mapping Agency, St. Louis, MO, USA, Jan. 2000.

[44] Shumate Jr., E. H., "The Radius of Curvature in the Prime Vertical," *ITEA Journal of Test and Evaluation*, Vol. 30, march 2009, pp. 159.

[45] Leica Geosystems AG, "LEICA SR520 GPS Geodetic Receiver," 1999.